

AD-A066 356

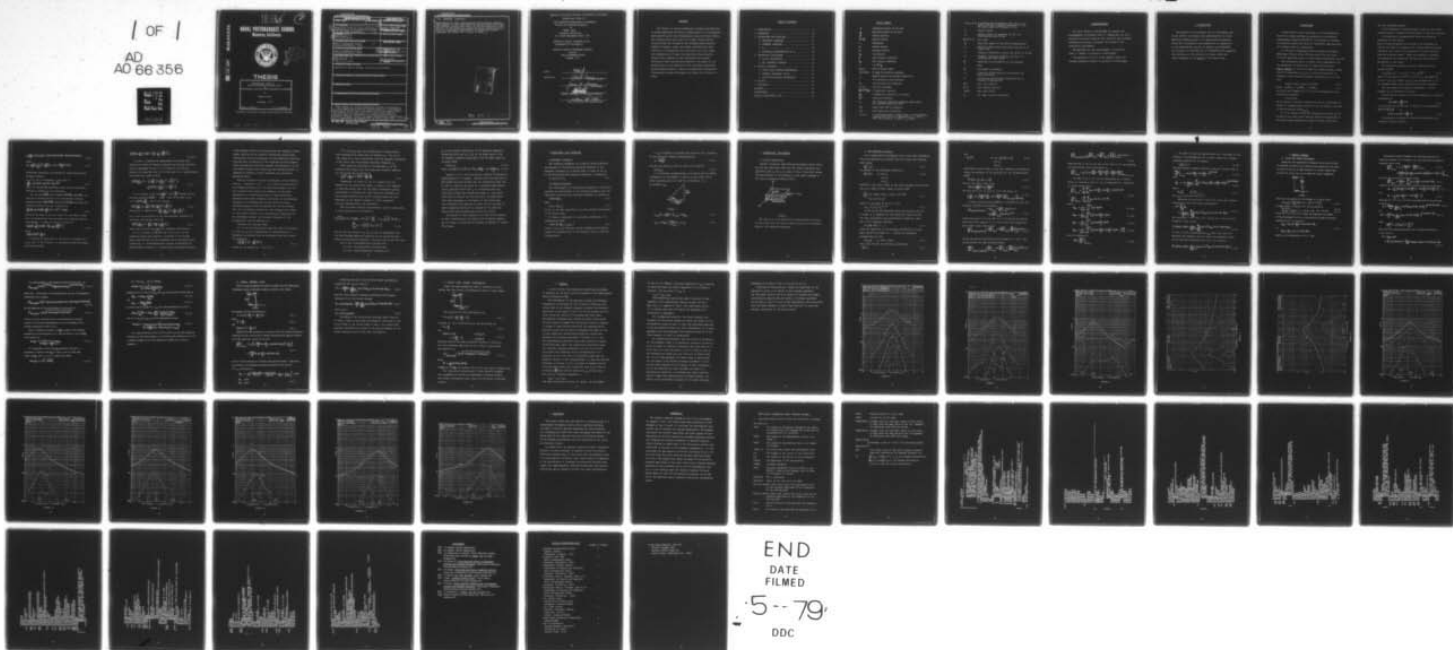
NAVAL POSTGRADUATE SCHOOL MONTEREY CALIF  
THEORETICAL STUDY OF FINITE AMPLITUDE STANDING WAVES IN RECTANG--ETC(U)  
DEC 78 M AYDIN

F/G 20/1

UNCLASSIFIED

NL

/ OF /  
AD  
A0 66 356



END  
DATE  
FILMED

5-79

DDC

AD A0 66356

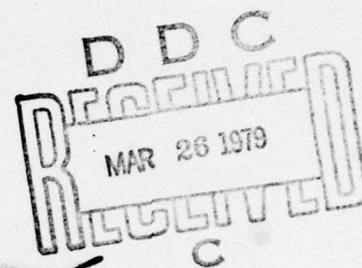
DDC FILE COPY

LEVEL II

2

# NAVAL POSTGRADUATE SCHOOL

Monterey, California



## THESIS

THEORETICAL STUDY OF  
FINITE AMPLITUDE STANDING WAVES  
IN  
RECTANGULAR CAVITIES WITH PERTURBED BOUNDARIES

by

Mehmet Aydin

December 1978

Thesis Advisor:

A. B. Coppens

Approved for public release; distribution unlimited.

79 03 26 059

UNCLASSIFIED

SECURITY CLASSIFICATION OF THIS PAGE (When Data Entered)

REPORT DOCUMENTATION PAGE		READ INSTRUCTIONS BEFORE COMPLETING FORM
1. REPORT NUMBER	2. GOVT ACCESSION NO.	3. RECIPIENT'S CATALOG NUMBER
4. TITLE (and Subtitle)		5. TYPE OF REPORT & PERIOD COVERED
6. Theoretical Study of Finite Amplitude Standing Waves in Rectangular Cavities with Perturbed Boundaries,		Master's Thesis 95 December 1978
7. AUTHOR(s)		8. PERFORMING ORG. REPORT NUMBER
10. Mehmet Aydin		9. CONTRACT OR GRANT NUMBER(s)
9. PERFORMING ORGANIZATION NAME AND ADDRESS		10. PROGRAM ELEMENT, PROJECT, TASK AREA & WORK UNIT NUMBERS
Naval Postgraduate School Monterey, California 93940		
11. CONTROLLING OFFICE NAME AND ADDRESS		12. REPORT DATE
Naval Postgraduate School Monterey, California 93940		December 1978
14. MONITORING AGENCY NAME & ADDRESS (if different from Controlling Office)		13. NUMBER OF PAGES
12. 64 p.		60
		15. SECURITY CLASS. (of this report)
		Unclassified
		15a. DECLASSIFICATION/DOWNGRADING SCHEDULE
16. DISTRIBUTION STATEMENT (of this Report)		
Approved for public release; distribution unlimited.		
17. DISTRIBUTION STATEMENT (of the abstract entered in Block 20, if different from Report)		
18. SUPPLEMENTARY NOTES		
19. KEY WORDS (Continue on reverse side if necessary and identify by block number)		
20. ABSTRACT (Continue on reverse side if necessary and identify by block number)		
<p>The effects of various geometrical boundary perturbations on finite-amplitude acoustical standing waves in a rectangular, rigid-walled cavity were investigated using non-linear theory. The standing waves that exist in an ideal cavity must be corrected when the boundaries are irregular. Three specific examples (stepped, linear and wedged perturbations) were worked out to demonstrate the corrections (in first order) near</p>		

DD FORM 1473

1 JAN 73

EDITION OF 1 NOV 68 IS OBSOLETE  
S/N 0102-014-6601

UNCLASSIFIED

SECURITY CLASSIFICATION OF THIS PAGE (When Data Entered)

1

251 450

over







Approved for public release; distribution unlimited.

Theoretical Study of  
Finite Amplitude Standing Waves in Rectangular  
Cavities with Perturbed Boundaries

by

Mehmet Aydın

Lieutenant, Turkish Navy

B.S., Naval Postgraduate School, 1978

Submitted in partial fulfillment of the  
requirements for the degree of

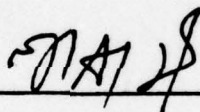
MASTER OF SCIENCE IN ENGINEERING ACOUSTICS

from the

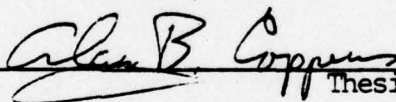
NAVAL POSTGRADUATE SCHOOL

December 1978

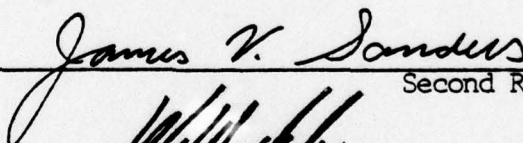
Author



Approved by:



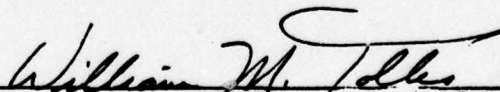
Thesis Advisor



Second Reader



Chairman, Department of Physics and Chemistry



Dean of Science and Engineering

## ABSTRACT

The effects of various geometrical boundary perturbations on finite-amplitude acoustical standing waves in a rectangular, rigid-walled cavity were investigated using non-linear theory. The standing waves that exist in an ideal cavity must be corrected when the boundaries are irregular. Three specific examples (stepped, linear and wedged perturbations) were worked out to demonstrate the corrections (in first order) near degeneracies for small perturbations. Those specific examples were compared to the experiments. The present theoretical model qualitatively predicts the effect of the perturbations on the behavior of the nonlinearly generated second harmonic. However, there are unexplained quantitative discrepancies between experiment and theory for a couple of cases.

## TABLE OF CONTENTS

1. INTRODUCTION .....	9
2. BACKGROUND .....	10
3. DEFINITIONS AND NOTATIONS .....	17
A. FREQUENCY PARAMETER .....	17
B. STRENGTH PARAMETER .....	17
C. $e_n$ .....	18
D. PICTORIAL REPRESENTATION OF $F_n$ .....	18
4. THEORETICAL DEVELOPMENT .....	19
A. CAVITY DESCRIPTION .....	19
B. THE PERTURBED BOUNDARY .....	20
5. SPECIFIC EXAMPLES .....	24
A. CAVITY WITH STEPPED PERTURBATION .....	24
B. LINEARLY PERTURBED CAVITY .....	28
C. CAVITY WITH WEDGED PERTURBATION .....	30
6. RESULTS .....	31
7. CONCLUSION .....	45
APPENDIX A .....	46
BIBLIOGRAPHY .....	58
INITIAL DISTRIBUTION LIST .....	59



# LIST OF SYMBOLS

$\rho$	Instantaneous density of the fluid
$\rho_0$	Equilibrium density of the fluid
$\Phi$	Velocity potential
$\vec{u} = \nabla \Phi$	Particle velocity
$s$	Condensation
$\nabla$	Gradient operator
$\nabla \cdot$	Divergence operator
$\nabla \times$	Curl operator
$\eta$	Shear viscosity coefficient
$\eta_B$	Bulk viscosity coefficient
$b$	$(4/3)\eta/\eta_B$
$\gamma = C_p/C_v$	Ratio of specific heats
$C_0^2 = (dP/d\rho)$	At $\rho = \rho_0$ for acoustical processes
$C_0$	Speed of sound in an unbounded volume of air
$P$	Instantaneous total pressure
$P_0$	Equilibrium total pressure
$p = P - P_0$	Acoustic pressure
$\square^2 = \nabla^2 - \partial^2/\partial t^2$	D'Lambertian operator
$\square_L^2$	D'Lambertian operator with losses
$\nabla^2$	Laplacian operator
$c_p$	The frequency dependent apparent phase speed for standing waves in cavity
RHS	Right hand side of equation
LHS	Left hand side of equation
$(n, m, l)$	A (time-independent) normal mode of a rectangular, rigid-walled cavity of dimensions $L_x, L_y$ and $L_z$ such that $k_x = n\pi/L_x$ , $k_y = m\pi/L_y$ , $k_z = l\pi/L_z$

$(n,m,l/w,\theta)$	A standing wave designation when the $(n,m,l)$ mode is driven at angular frequency $w$ ; $\theta$ is the phase angle with respect to $t=0$ .
$Q$	Quality factor
$Q_n$	Quality factor at resonance of the $n$ th standing wave when driven
$\beta = (\gamma + 1)/2$	For a gas
$M_0$	Peak Mach number of the driven standing wave
$C_n$	Effective phase speed associated with the $n$ th normal mode
$w$	(Angular) frequency at which the cavity is driven
$w_n$	(Angular) resonance frequency of the $n$ th standing wave when driven
$\Delta$	Magnitude of perturbation on the boundary
$t$	Time
$\epsilon$	Perturbation parameter
$p_0$	Classical linear solution for pressure for ideal boundaries
$p'$	First-order perturbation correction due to boundary irregularities
$1(t)$	Unit step function
$\delta(t)$	Unit impulse function
$\text{Re}\{ \}$	Real part of $\{ \}$
$a_0$	0th order Fourier coefficient

### ACKNOWLEDGEMENT

The autor wishes to acknowledge the support and encouragement of Professor Alan B. Coppens, who not only provided the initial idea for the topic, but also provided invaluable assistance throughout the course of the theoretical development.

The generous aid and encouragement of Professor James V. Sanders is gratefully acknowledged.

The generous aid of LT. Resai Çağlayan about the Versatec graphical process is gratefully acknowledged.



## 1. INTRODUCTION

The purpose of this research was to investigate some of the effects of boundary wall perturbations on finite amplitude standing waves in a rigid-walled rectangular cavity. The investigation was prompted by an examination of the experimental results of Coppens and Sanders[3], the research of DeVall[5] and of Kilmer[4], which suggested the existence of the excitation of modes other than those belonging to the family of the driven mode.

## 2. BACKGROUND

A plane elastic wave travelling in a non-dissipative fluid will change waveform as predicted by the relevant hydrodynamic equations [6],[7]. If the problem is extended to absorptive media, only waves of relatively high amplitude will change waveforms appreciably.

At the Naval Postgraduate School, Coppens and Sanders [3], Kilmer [4], and DeVall [5] have dealt with the study of finite amplitude waves in rigid-walled rectangular cavities.

One interesting result of these cavity experiments was the appearance of excitations of modes which were not family members of the driven mode. For example, assume a rigid cavity of dimensions  $L_x, L_y, L_z$  is driven acoustically at frequency  $w$ , the resultant pressure standing wave is of the form

$$\cos k_x x \cos k_y y \cos k_z z \cos(wt + \theta) \quad (2.1)$$

$$\text{where } k_x = N\pi/L_x, \quad k_y = M\pi/L_y, \quad k_z = L\pi/L_z \quad (2.2)$$

and  $N, M, L$  are integers. Eq. (2.1) can be represented by the notational shorthand

$$(N, M, L/w, \theta)$$

If the cavity is driven to excite the  $(0, M, 0)$  mode, then the family of standing waves consist of all of those of the form  $(0, nM, 0/nw, \theta_n)$  when  $nw \approx w_{0, M, 0}$ .

As it is stated in [3], "The standing waves which can be excited in any real cavity deviate from the predictions of the linear wave equation with ideal boundary conditions

"for the following reasons:

(a).The presence of boundary-layer losses at the cavity surfaces yields a dispersive contribution to the wave equation.

(b).Geometrical irregularities alter the effective dimensions of the cavity.

Both of these mechanism can be treated as equivalent as long as the shift in frequency are so small that the actual resonances are close to the theoretical values resulting from the classical model." These are treated by assuming the dimensions are exact, and the apparent phase speed is determined on that basis.

The resonance frequency for each standing wave is defined as [3]

$$w_n = C_n [(n_x k_x)^2 + (n_y k_y)^2 + (n_z k_z)^2]^{1/2} \quad (2.3)$$

where k's are given by Eq.(2.2) and n is a shorthand for the set  $(n_x, n_y, n_z)$  where  $n_x, n_y, n_z$  are integers, and  $C_n$  is the apparent phase speed appropriate for that frequency.

The non-linear wave equation applicable to this problem can be obtained as follows:

The continuity equation for wave propagation in Eulerian coordinates is

$$\nabla \cdot (\rho \vec{u}) + \frac{\partial \rho}{\partial t} = 0 \quad (2.4)$$

this equation can be written in terms of the condensation,

$$s \equiv (\rho - \rho_0) / \rho_0 \quad \text{as}$$

$$\nabla \cdot [(1+s) \vec{u}] + \frac{\partial s}{\partial t} = 0 \quad (2.5)$$

The equation of motion in Eulerian coordinates for a contained viscous fluid is



$$\rho \left[ \frac{\partial \vec{u}}{\partial t} + (\vec{u} \cdot \nabla) \vec{u} \right] = -\nabla P + b\gamma \nabla(\nabla \cdot \vec{u}) - \gamma \nabla \times \nabla \times \vec{u} + \text{ODAT} \quad (2.6)$$

where

$$P = \frac{\rho c_0^2}{\gamma} \left( \frac{\rho}{\rho_0} \right)^\gamma \doteq \frac{\rho c_0^2}{\gamma} \left[ 1 + \gamma s + \frac{\gamma(\gamma-1)}{2} s^2 \right] \quad (2.7)$$

ODAT=Other dispersive and absorptive terms arising from boundary effects.

Eq.(2.6) can be rearrange in the form of

$$\frac{\partial \vec{u}}{\partial t} + (\vec{u} \cdot \nabla) \vec{u} + \frac{1}{\rho} \nabla P = \frac{1}{\rho} \mathcal{L} \vec{u} \quad (2.8)$$

where the operator  $\mathcal{L}$  describes those physical processes leading to absorption and dispersion.

One can write  $\nabla \times \vec{u} = 0$  and therefore  $\vec{u} = \nabla \Phi$ , where  $\Phi$  is the velocity potential, based on the irrotational velocity assumption. Hence,  $\mathcal{L} \vec{u} = \mathcal{L} \nabla \Phi$ . Replacing  $\vec{u} = \nabla \Phi$  and using the condensation, Eq.(2.8) can be written as

$$\frac{\partial}{\partial t} \nabla \Phi + \frac{1}{2} \nabla (\nabla \Phi)^2 + \frac{c_0^2}{\gamma-1} \nabla (1+s)^{\gamma-1} = \nabla \mathcal{L} \Phi \quad (2.9)$$

Now, with the help of Eq.(2.5) and (2.9), and after a good deal of manipulation the non-linear wave equation may be approximated in terms of velocity potential

$$c_p^2 \square^2 \Phi \doteq \frac{\partial}{\partial t} \left[ (\nabla \Phi)^2 + \frac{\gamma-1}{2} \frac{1}{c_0^2} \left( \frac{\partial \Phi}{\partial t} \right)^2 \right] \quad (2.10)$$

where

$$c_p^2 \square^2 \equiv c_0^2 \square^2 + \frac{\partial}{\partial t} \mathcal{L}$$

It should be noted that if the fluid is lossless and  $c_p = c_0$  then (2.10) reduces to a previously known non-linear wave equation [9]

$$c_0^2 \square^2 \Phi \doteq \frac{\partial}{\partial t} [(\nabla \Phi)^2 + \frac{\gamma-1}{2} \frac{1}{c_0^2} \left(\frac{\partial \Phi}{\partial t}\right)^2] \quad (2.10a)$$

In order to express the approximate non-linear wave equation in terms of acoustic pressure and particle velocity, one can rearrange the Eq.(2.9) in terms of  $p$  and  $\vec{u}$  and combine that equation with (2.10). The result is a quadratically non-linear wave equation [2]

$$\begin{aligned} c_p^2 \square_L^2 \left(\frac{p}{\rho_0 c_0^2}\right) \doteq & -\frac{1}{2} \frac{\partial^2}{\partial t^2} \left[ \gamma \left(\frac{p}{\rho_0 c_0^2}\right)^2 + \left(\frac{\vec{u}}{c_0}\right)^2 \right] \\ & + \frac{1}{2} c_0^2 \nabla^2 \left[ \left(\frac{p}{\rho_0 c_0^2}\right)^2 - \left(\frac{\vec{u}}{c_0}\right)^2 \right] \end{aligned} \quad (2.11)$$

If it chances to be that  $\left(\frac{p}{\rho_0 c_0^2}\right)^2$  and  $\left(\frac{\vec{u}}{c_0}\right)^2$  nearly satisfy the wave equation,  $c_0^2 \square^2(\quad) = 0$ , then on the RHS of Eq.

(2.11)  $c_0^2 \nabla^2 \doteq \frac{\partial^2}{\partial t^2}$  and (2.11) becomes

$$c_p^2 \square_L^2 \left(\frac{p}{\rho_0 c_0^2}\right) \doteq -\frac{\partial^2}{\partial t^2} \left[ \frac{\gamma-1}{2} \left(\frac{p}{\rho_0 c_0^2}\right)^2 + \left(\frac{\vec{u}}{c_0}\right)^2 \right] \quad (2.12)$$

Further, if it happens that  $\frac{\partial^2}{\partial t^2} \left(\frac{p}{\rho_0 c_0^2}\right)^2 \doteq \frac{\partial^2}{\partial t^2} \left(\frac{\vec{u}}{c_0}\right)^2$ ,

as is true for solutions to the wave equation separated in cartesian coordinates, then [2]

$$c_p^2 \square_L^2 \left(\frac{p}{\rho_0 c_0^2}\right) \doteq -\frac{\partial^2}{\partial t^2} \left[ \frac{\gamma+1}{2} \left(\frac{p}{\rho_0 c_0^2}\right)^2 \right] \quad (2.13)$$

(Note that this is true only for cartesian coordinates.)

As it is stated in [3] "The LHS of Eq.(2.13) is the classical, linear wave equation pertinent to the system under study. The RHS can be interpreted as a forcing function consisting of a three-dimensional spatial distribution of phase-coherent sources. In a second-order perturbation theory,

"this forcing function is obtained from the classical (first-order) solution of the acoustic problem. The second-order perturbation solution describes the nonlinearities resulting from the self interaction of the classical solution. Higher-order perturbation solutions consider the interaction of the non-linear solution with itself, and the forcing function is composed of products of both classical and nonlinearly generated terms.

Thus, if a system is driven at frequency  $w$ , the nonlinear term in... "equation (2.13) "... will force the existence of all integer multiples  $nw$  of the driving frequency and the full solution must contain all harmonics of the input frequency. In a closed cavity, each of those nonlinearly generated waves whose frequency lies close to the resonance frequency of a standing wave of the cavity and whose associated spatial function matches that of the standing wave can be strongly excited. Just how strongly will depend on the quality factor  $Q$  for the particular resonance and the difference between the resonance frequency of the standing wave and the harmonic  $nw$ .....

"Consider two limiting cases.

"(1) If the forcing function does not have its frequency  $nw$  close to  $w_n$ , this standing wave is being forced at a frequency far removed from its resonance. Since this yields the inequality

$$|C_0^2 \bar{\sigma}_p^2| \gg \left| \frac{\partial}{\partial t} \mathcal{L}_p \right| \quad (2.14)$$

losses can be ignored in..."Eq.(2.13).



"(2) If  $n\omega \sim \omega_n$ , then the standing wave is being forced near resonance, and losses must be retained in..."Eq.(2.13).

"The value of  $C_n$  can be determined from the apparent dimensions of the cavity and the measured resonance frequency  $\omega_n$ .

"The losses are described by the measured  $Q_n$  of the resonance. This means that the linear-wave equation operator for the system can be written as

$$C_0^2 \square^2 + \frac{\partial}{\partial t} L \doteq C_n^2 \square^2 - \frac{n\omega}{Q_n} \frac{\partial}{\partial t} \quad (2.15)$$

"Comparison of cases (1) and (2) reveals that the response of the cavity when  $n\omega \not\sim \omega_n$  is order of  $1/Q$  compared to that when  $n\omega \sim \omega_n$ . Thus for the high- $Q$  resonances usually encountered in cavities with rigid walls, the components in the forcing function which excite standing waves far from resonance can be ignored compared to those components exciting standing waves near resonance....

"The non-linear, coupled, transcendental equation applicable to this problem can be expressed as

$$R_n \begin{Bmatrix} \cos \\ \sin \end{Bmatrix} (\phi_n - \theta_n) = N_0 M_0 Q_n \cos \theta_n \left[ \frac{1}{2} \sum_{j=1}^{n-1} R_j R_{n-j} \begin{Bmatrix} \cos \\ \sin \end{Bmatrix} (\phi_j + \phi_{n-j}) - \sum_{j=1}^{\infty} R_{n+j} R_j \begin{Bmatrix} \cos \\ \sin \end{Bmatrix} (\phi_{n+j} - \phi_j) \right] \quad (2.16)$$

for all  $n > 1$ . The values of  $Q_n$  and  $\omega_n$  must be determined from the infinitesimal-amplitude behavior of the cavity. The Mach number  $M_0$  and driving frequency  $\omega$  are known and  $N_0$  has the value

$N_0 = 1/2$  for a one-dimensional standing wave

$1/4$  for a two-dimensional standing wave

$1/8$  for a three-dimensional standing wave."

$R_n$  is the Fourier coefficient of  $n$ th harmonic component, normalized such that  $R_1=1$ .  $\phi_n$  is the phase angle of the  $n$ th harmonic component, where  $\phi_1=0$ , and the phase angle  $\theta_n$  is given by [3]

$$\tan \theta_n = -F_n \quad (2.17)$$

$$\text{where } F_n = Q_n \left[ (nw)^2 - w_n^2 \right] / (nw)^2 \approx 2Q_n \left( \frac{nw - w_n}{w_n} \right) \text{ for } \frac{nw - w_n}{w_n} \ll 1 \quad (2.18)$$

Equation (2.16) can be solved by a method of successive approximations on a digital computer. This has been done by [3] and [5] and both decided that the theoretical model can be used to identify the modes of a non-ideal, rigid-walled cavity provided quantities  $e_n$  to be defined later are sufficiently small. The theoretical model in its present form fails to account for the excitation of modes other than those belonging to the family of the driven mode. This excitation was observed to occur only in the case of nearly degenerate modes. It is believed to be caused by some linear coupling mechanism within the cavity.

The purpose of this research is to see if the presence of wall irregularities can explain how non-family members may be strongly excited, and to present an example to support this theory.

### 3. DEFINITIONS AND NOTATIONS

#### A. FREQUENCY PARAMETER

The frequency parameter is a quantity which indicates the position of the driving frequency relative to the resonance frequency,  $f_1$ , of driven mode in terms of the  $Q_1$  of the driven mode. The frequency parameter is defined by

$$F_1 = 2Q_1(f - f_1)/f_1 \quad (3.1)$$

#### B. STRENGTH PARAMETER

The investigation of the pressure waveform in the cavity required the calculation of the strength parameter from the observable quantities. The strength parameter is defined as

$$\text{STRPM} = M_0 P Q_1 \quad (3.2)$$

where

$$M_0 = P_1 / (\rho_0 C_0^2) \quad (3.3)$$

and  $P_1$  is the peak amplitude of  $p_1$ , the pressure distribution of the driven mode.

In terms of observable or calculable quantities it is reformulated as [5]

$$\text{STRPM} = \sqrt{2} V P Q_1 / (S_m \rho C_0)^2 \quad (3.4)$$

where  $V$  and  $S_m$  are the rms voltage reading and microphone sensitivity respectively of the receiver used to sense the standing wave.



C.  $e_n$  is defined to indicate the position of  $w_n$  relative to the classical harmonic frequencies,  $nw_1$ .

$$e_n = \frac{w_n - nw_1}{nw_1} \quad (3.5)$$

and one can relate  $e_n$  with  $F_n$  from (2.18) such as

$$F_n \doteq 2Q_n e_n \quad (3.6)$$

D. A pictorial representation of  $F_n$  which will be useful throughout the development is given in Fig.1. From now on three subscripts will be used for convenience. i.e.

$F_n$  becomes  $F_{nml}$ .

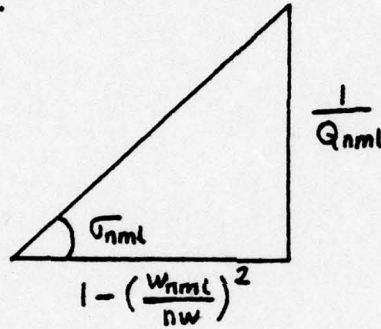


FIGURE 1

$$F_{nml} = \left[ 1 - \left( \frac{w_{nml}}{nw} \right)^2 \right] Q_{nml} = \cot \sigma_{nml} \quad (3.7)$$

$$Q_{nml} \sin \sigma_{nml} = \frac{Q_{nml}}{(1 + F_{nml}^2)^{1/2}} = S_{nml} \quad (3.8)$$

#### 4. THEORETICAL DEVELOPMENT

##### A. CAVITY DESCRIPTION

Assume a perfectly rigid-walled rectangular cavity which has one wall perturbed such that the cavity dimensions are  $L_x[1 + \epsilon f(y,z)]$ ,  $L_y$  and  $L_z$  as shown in Fig.2 below. Also assume the perturbation on the boundary is very small compared to the cavity dimensions,  $|\epsilon f(y,z)| \ll 1$ .

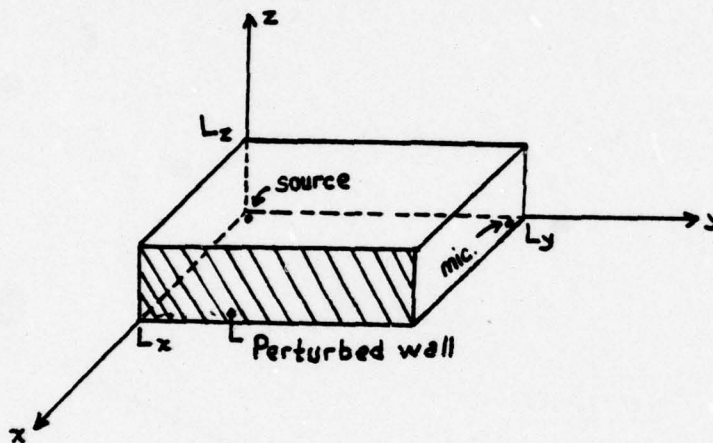


FIGURE 2

The cavity is to be excited by a source near the origin in such a way that the (N,M,L) mode is driven at a frequency close to its resonance frequency.

## B. THE PERTURBED BOUNDARY

For a rigid-walled rectangular cavity with ideal boundaries ( $\epsilon=0$ ), the pressure  $p_0$  obtained from the linear wave equation with losses

$$\square_L^2 p_0 = 0 \quad (4.1)$$

is subject to the following conditions,

$$\begin{aligned} \nabla p_0 \cdot \vec{n} = 0 \quad & \text{at } x=0, L_x \\ & y=0, L_y \\ & z=0, L_z \end{aligned} \quad (4.2)$$

where  $\vec{n}$  is the local normal to the ideal boundary. The solution for  $p_0$  in terms of Mach number is given by [4]

$$\begin{aligned} \frac{p_0}{\rho_0 c_0^2} &= M_0 \cos k_x x \cos k_y y \cos k_z z \cos(\omega t + \theta) \\ &= M_0 (N, M, L/w, \theta) \end{aligned} \quad (4.3)$$

where  $k$ 's are given in Eq.(2.2), and

$$w = c_p (k_x^2 + k_y^2 + k_z^2)^{1/2} \quad (4.4)$$

If the cavity has perturbed walls, the solution will be in terms of a summation of the classical linear solution for ideal boundaries plus perturbation correction terms due to the irregular boundary:

$$p = p_0 + \epsilon p' + \epsilon^2 p'' + \dots \quad (4.5)$$

Since the magnitude of the boundary perturbation is kept small, second and higher terms in  $\epsilon$  can be considered insignificant, so that

$$p = p_0 + \epsilon p' \quad (\text{to first order}) \quad (4.6)$$

and  $p$  must satisfy the following conditions,

$$\square^2 p = 0 \quad (4.7)$$



and

$$\begin{aligned} \nabla p \cdot \vec{n} &= 0 & \text{at } x=0, L_x [1+\epsilon f(y,z)] & \quad (4.8) \\ & & y=0, L_y & \\ & & z=0, L_z & \end{aligned}$$

where  $\vec{n}$ , the local normal to the real surface, is obtained by taking the gradient of the equation for the boundary, given by [2]

$$\vec{n} = \nabla \{x - L_x [1 + \epsilon f(y, z)]\} \quad (4.10)$$

Thus, to the first order in  $\epsilon$ ,

$$\vec{n} = \hat{x} - \epsilon L_x \frac{\partial f(y, z)}{\partial y} \hat{y} - \epsilon L_x \frac{\partial f(y, z)}{\partial z} \hat{z} \quad (4.11)$$

and when Eq. (4.11) is used in (4.8) the result is

$$\left[ \frac{\partial p}{\partial x} - \epsilon L_x \frac{\partial f(y, z)}{\partial y} \frac{\partial p}{\partial y} - \epsilon L_x \frac{\partial f(y, z)}{\partial z} \frac{\partial p}{\partial z} \right]_{x=L_x [1+\epsilon f(y, z)]} = 0 \quad (4.12)$$

A Taylor series expansion [4] for  $p$  evaluated at the real boundary  $L_x [1 + \epsilon f(y, z)]$  produces

$$\begin{aligned} p|_{x=L_x [1+\epsilon f(y, z)]} &= p|_{x=L_x} + \frac{\partial p}{\partial x} \Big|_{x=L_x} \epsilon L_x f(y, z) \\ &+ \frac{1}{2} \frac{\partial^2 p}{\partial x^2} \Big|_{x=L_x} [\epsilon L_x f(y, z)]^2 + \dots \quad (4.13) \end{aligned}$$

Substituting Eq. (4.6) into RHS of (4.13), taking the partial derivative with respect to  $x$  on both sides and keeping the first-order terms in  $\epsilon$ , yields

$$\frac{\partial p}{\partial x} \Big|_{x=L_x [1+\epsilon f(y, z)]} = \frac{\partial p_0}{\partial x} \Big|_{x=L_x} + \epsilon \frac{\partial p'}{\partial x} \Big|_{x=L_x} + \frac{\partial^2 p_0}{\partial x^2} \Big|_{x=L_x} \epsilon L_x f(y, z) + \dots \quad (4.14)$$

Taking the partial derivatives with respect to  $y$  and  $z$  and using exactly the same procedure gives

$$\frac{\partial p}{\partial y} \Big|_{x=L_x [1+\epsilon f(y, z)]} = \frac{\partial p_0}{\partial y} \Big|_{x=L_x} + \epsilon \frac{\partial p'}{\partial y} \Big|_{x=L_x} + \frac{\partial^2 p_0}{\partial y \partial x} \Big|_{x=L_x} \epsilon L_x f(y, z) + \dots \quad (4.15)$$

$$\left. \frac{\partial p}{\partial z} \right|_{x=L_x[1+\epsilon f(y,z)]} = \left. \frac{\partial p_0}{\partial z} \right|_{x=L_x} + \epsilon \left. \frac{\partial p'}{\partial z} \right|_{x=L_x} + \frac{\partial^2 p_0}{\partial z \partial x} \bigg|_{x=L_x} \epsilon L_x f(y,z) + \dots \quad (4.16)$$

Substituting (4.14), (4.15) and (4.16) into (4.12) and keeping the first-order terms in  $\epsilon$  results in

$$\left. \frac{\partial p'}{\partial x} \right|_{x=L_x} = L_x \left[ -f(y,z) \frac{\partial^2 p_0}{\partial x^2} + \frac{\partial f(y,z)}{\partial y} \frac{\partial p_0}{\partial y} + \frac{\partial f(y,z)}{\partial z} \frac{\partial p_0}{\partial z} \right]_{x=L_x} \quad (4.17)$$

The RHS of Eq.(4.17) can be represented as a Fourier series in cosines, so that  $p'$  can be expressed as a summation of normal modes. Hence,

$$\left. \frac{\partial p'}{\partial x} \right|_{x=L_x} = \sum_{m=0}^{\infty} \sum_{l=0}^{\infty} a_{ml} \cos \frac{m\pi}{L_y} y \cos \frac{l\pi}{L_z} z \cos(\omega t + \theta) \quad (4.18)$$

or

$$\left. \frac{\partial p'}{\partial x} \right|_{x=L_x} = \sum_{m=0}^{\infty} \sum_{l=0}^{\infty} a_{ml} (0, m, l / \omega, \theta)$$

where

$$a_{00} = \frac{1}{L_y L_z} \int_0^{L_y} \int_0^{L_z} [G] dy dz \quad (4.19a)$$

$$a_{m0} = \frac{2}{L_y L_z} \int_0^{L_y} \int_0^{L_z} [G] \cos \frac{m\pi}{L_y} y dy dz \quad (4.19b)$$

$$a_{0l} = \frac{2}{L_y L_z} \int_0^{L_y} \int_0^{L_z} [G] \cos \frac{l\pi}{L_z} z dy dz \quad (4.19c)$$

$$a_{ml} = \frac{4}{L_y L_z} \int_0^{L_y} \int_0^{L_z} [G] \cos \frac{m\pi}{L_y} y \cos \frac{l\pi}{L_z} z dy dz, \quad m \neq 0, l \neq 0 \quad (4.19d)$$

and  $G$  is defined as

$$G \equiv \left. \frac{\partial p'}{\partial x} \right|_{x=L_x} \quad (4.19e)$$

In order to find the contribution to  $p'$  from each of the terms, it is stated [2] that for a cavity forced by a dynamic boundary condition at a boundary

$$c_p^2 \square_L^2 p' = 0 \quad (4.20)$$

and the dynamic boundary condition from the  $(m, l)$ th term is

$$\left. \frac{\partial p'_{ml}}{\partial x} \right|_{x=L_x} = A \cos \frac{m\pi}{L_y} y \cos \frac{l\pi}{L_z} z e^{i(\omega t + \theta)} \quad (4.21)$$

then

$$p'_{ml} = -A \frac{1}{\left(\frac{w}{c_0}\right)^2 L_x} \sum_{n=0}^{\infty} \Delta_n (-1)^n S_{nml} \cos \frac{n\pi}{L_x} x \cos \frac{m\pi}{L_y} y \cos \frac{l\pi}{L_z} z e^{i(\omega t + \theta + \sigma_{nml})} \quad (4.22)$$

where

$$\Delta_n = \begin{cases} 1 & \text{if } n=0 \\ 2 & \text{if } n=1, 2, 3, \dots \end{cases} \quad (4.23)$$

and  $S_{nml}$  is given by Eq.(3.8).

Applying this solution to Eq.(4.18) gives the complete solution for the first-order perturbation

$$p' = \sum_{\substack{m=0 \\ l=0}}^{\infty} p'_{ml} = -\frac{1}{\left(\frac{w}{c_0}\right)^2 L_x} \sum_{\substack{n=0 \\ m=0 \\ l=0}}^{\infty} a_{ml} \Delta_n (-1)^n S_{nml} (n, m, l / w, \theta + \sigma_{nml}) \quad (4.24)$$

and combining (4.24) with (4.6) yields the total acoustic pressure in the cavity.

$$p = (N, M, L / w, \theta) - \frac{\epsilon}{\left(\frac{w}{c_0}\right)^2 L_x} \sum_{\substack{n=0 \\ m=0 \\ l=0}}^{\infty} a_{ml} \Delta_n (-1)^n S_{nml} (n, m, l / w, \theta + \sigma_{nml}) \quad (4.25)$$

If this is near a resonance,  $w \sim w_{nml}$ , then this term will dominate the summation and all other non-degenerate terms can be omitted. Consequently, the Eq.(4.25) becomes

$$p = (N, M, L / w, \theta) - \frac{\epsilon}{\left(\frac{w}{c_0}\right)^2 L_x} a_{ml} \Delta_n (-1)^n S_{nml} (n, m, l / w, \theta + \sigma_{nml}) \quad (4.26)$$



## 5. SPECIFIC EXAMPLES

### A. CAVITY WITH STEPPED PERTURBATION

Assume that the rigid-walled rectangular cavity given in Fig.2 is perturbed as shown in Fig.3 below, and also assume that the cavity is driven in the  $(0,1,0)$  mode resulting  $(0,1,0/w,\theta)$  standing wave and that the  $(0,2,0)$  and  $(1,0,0)$  modes are (nearly) degenerate.

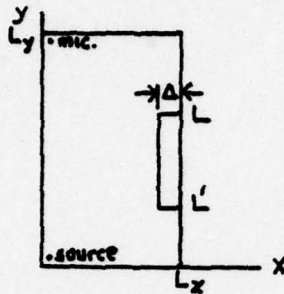


FIGURE 3

From Fig.3 the equation for the boundary at  $L_x$  can be found,

$$x = L_x \left\{ 1 - \frac{\Delta}{L_x} \left[ 1(y-L') - 1(y-L) \right] \right\} \quad (5A.1)$$

By means of Eq.(4.8)  $\epsilon$  and  $f(y,z)$  can be written as

$$\epsilon = \Delta/L_x \quad (5A.2)$$

$$f(y,z) = - \left[ 1(y-L') - 1(y-L) \right] \quad \text{at } L' < y < L \quad (5A.3)$$

Since the  $(0,2,0)$  and  $(1,0,0)$  modes are degenerate the emphasis of this development will be on these particular modes. The pressure distribution of  $(0,2,0)$  mode is

$$p_{020} = P_2 \cos \frac{2\pi}{L_y} y \cos(2\omega t + \theta_2)$$

or

$$p_{020} = P_2 (0, 2, 0 / 2\omega, \theta_2)$$

(5A.4)

where  $P_2$  is the amplitude of  $(0,2,0)$  mode.

Utilizing the theory developed in the preceeding sections and using the equations (4.17) through (4.26), the first-order perturbation correction can be found

$$\begin{aligned} \left. \frac{\partial p'}{\partial x} \right|_{x=L_x} &= L_x \left[ \frac{\partial f(y,z)}{\partial y} \frac{\partial p_{020}}{\partial y} \right]_{x=L_x} \\ &= \frac{2\pi P_2 L_x}{L_y} \left\{ \left[ \sin \frac{2\pi}{L_y} y \cos(2\omega t + \theta_2) \right] \left[ \delta(y-L') - \delta(y-L) \right] \right\}_{x=L_x} \end{aligned} \quad (5A.5)$$

Eq.(5A.5) can be written as a Fourier series

$$\left. \frac{\partial p'}{\partial x} \right|_{x=L_x} = \frac{2\pi P_2 L_x}{L_y} \sum_{m=0}^{\infty} a_m \cos \frac{m\pi}{L_y} y \cos(2\omega t + \theta_2) \quad (5A.6)$$

Inversion of the Eq.(5A.5) and (5A.6) yields the Fourier coefficients

$$a_m = \frac{2}{L_y} \left[ \sin\left(\frac{2\pi}{L_y} L'\right) \cos\left(\frac{m\pi}{L_y} L'\right) - \sin\left(\frac{2\pi}{L_y} L\right) \cos\left(\frac{m\pi}{L_y} L\right) \right] \quad (5A.7)$$

and

$$a_0 = \frac{1}{L_y} \left[ \sin\left(\frac{2\pi}{L_y} L'\right) - \sin\left(\frac{2\pi}{L_y} L\right) \right] \quad (5A.8)$$

Recalling Eq.(4.23) and (4.24), first order perturbation correction,  $p'$ ,

is found as

$$p' = -\frac{2\pi P_2 L_x}{L_y} \frac{a_0}{\left(\frac{2\omega}{c_0}\right)^2 L_x} (2)(-1)^1 Q_{100} \sin \sigma_{100} \cos \frac{\pi x}{L_x} e^{i(2\omega t + \theta_2 + \sigma_{100})} \quad (5A.9)$$

and

$$\epsilon p' = \frac{4\pi P_2}{L_y} \epsilon a_0 \frac{1}{\left(\frac{2\omega}{c_0}\right)^2} Q_{100} \sin \sigma_{100} \cos \frac{\pi x}{L_x} e^{i(2\omega t + \theta_2 + \sigma_{100})} \quad (5A.10)$$

where

$$\left(\frac{2\omega}{c_0}\right)^2 = (2k_{100})^2 = \left(\frac{4\pi}{L_y}\right)^2$$

Hence, the total pressure, associated with the angular frequency  $2\omega$ ,

in the cavity is

$$\begin{aligned} p &= p_{020} + \epsilon p' \\ &= p_2(0, 2, 0/2\omega, \theta_2) + \frac{P_2 L_y}{4\pi} \epsilon a_0 Q_{100} \sin \sigma_{100} (1, 0, 0/2\omega, \theta_2 + \sigma_{100}) \end{aligned} \quad (5A.11)$$

The total pressure at the microphone position,  $x=0$  and  $y=L_y$ , is

$$P|_{\text{mic. position}} = P_2 \operatorname{Re} \left\{ e^{i(2\omega t + \theta_2)} + \left[ \frac{L_y}{4\pi} \epsilon d_0 Q_{100} \sin \sigma_{100} \right] e^{i(2\omega t + \theta_2 + \sigma_{100})} \right\} \quad (5A.12)$$

Define  $B = [ \quad ]$  and after a little manipulation and use of trigonometric identities, (5A.12) becomes

$$P|_{\text{mic. position}} = P_2 \left\{ (1 + B \cos \sigma_{100}) \cos(2\omega t + \theta_2) - (B \sin \sigma_{100}) \sin(2\omega t + \theta_2) \right\} \quad (5A.13)$$

and the amplitude of the total pressure in the cavity is

$$P|_{\text{mic. position}} = P_2 \sqrt{(1 + B \cos \sigma_{100})^2 + (B \sin \sigma_{100})^2} \quad (5A.14)$$

Eq.(5A.14) is the corrected value of the amplitude of the second harmonic of the driving mode, obtained by Eq.(2.16), because of the boundary irregularity given in Fig.3.

Now, it is desired to express  $\sin \sigma_{100}$  in terms of the frequency parameter of the driving mode, (0,1,0). With the help of Fig.1,  $\sin \sigma_{100}$  can be written as

$$\sin \sigma_{100} = \frac{1}{\left\{ 1 + Q_{100}^2 \left[ 1 - \left( \frac{f_{100}}{2f} \right)^2 \right]^2 \right\}^{1/2}} \quad (5A.15)$$

If  $f$  approaches to zero then  $\sigma_{100}$  approaches to  $\pi$ , and if  $f$  approaches to infinity then  $\sigma_{100}$  is close to zero. In these same limits  $\cos \sigma_{100}$  goes to  $-1$  and  $+1$  respectively. Hence

$$\cos \sigma_{100} = \pm \sqrt{1 - \sin^2 \sigma_{100}} \quad (5A.16)$$



For  $2f \sim f_{100}$ , (5A.15) becomes

$$\sin \sigma_{100} \doteq \frac{1}{\left\{ 1 + \left( 2Q_{100} \frac{2f - f_{100}}{f_{100}} \right)^2 \right\}^{1/2}} \quad (5A.17)$$

Recalling Eq.(3.1) and (3.5),  $F_{100}$  and  $e_{100}$  can be written in the form of

$$F_{010} = 2Q_{010} \frac{f - f_{010}}{f_{010}} \quad (5A.18)$$

and

$$e_{100} = \frac{f_{100} - 2f_{010}}{2f_{010}} \quad (5A.19)$$

Eq.(5A.19) can be solved for  $f_{100}$  and this substituted into (5A.17)

$$2Q_{100} \frac{2f - f_{100}}{f_{100}} = 2Q_{010} \frac{Q_{100}}{Q_{010}} \frac{f - f_{010}(1 + e_{100})}{f_{010}(1 + e_{100})} \quad (5A.20)$$

Use of  $1/(1+e_{100}) \doteq 1-e_{100}$  and little manipulation reveals

$$\sin \sigma_{100} \doteq \frac{1}{\sqrt{1 + \left\{ \frac{Q_{100}}{Q_{010}} [F_{010} - 2Q_{010} e_{100}] (1 - e_{100}) \right\}^2}} \quad (5A.21)$$

As a result, equations (5A.14), (5A.16), (5A.21) are the final amplitude correction of the second harmonic of the driving mode obtained by Eq.(2.16) .

A computer program for this was developed by author and is given in appendix A.

## B. LINEARLY PERTURBED CAVITY

Using the same assumptions in section A, assume that the rigid-walled rectangular cavity is perturbed linearly as shown in Fig.4 below.

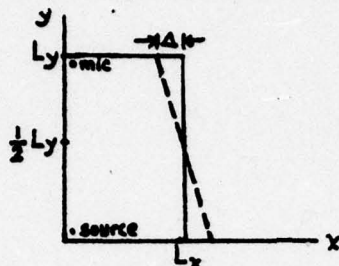


FIGURE 4

The equation for this perturbation is

$$x = L_x \left[ 1 + \frac{\Delta}{L_x} \left( 1 - \frac{2}{L_y} y \right) \right] \quad (5B.1)$$

Hence,

$$\epsilon = \frac{\Delta}{L_x} \quad (5B.2)$$

and

$$f(y,z) = \left( 1 - \frac{2}{L_y} y \right) \quad (5B.3)$$

Applying the same procedure as in section A, the first-order perturbation correction and the total acoustic pressure associated with angular frequency  $2\omega$  in that particular cavity can be found

$$\begin{aligned} \left. \frac{\partial p'}{\partial x} \right|_{x=L_x} &= L_x \left\{ \left[ -\frac{2\pi P_2}{L_y} \sin \frac{2\pi}{L_y} y \cos(2\omega t + \theta_2) \right] \left( -\frac{2}{L_y} \right) \right\} \\ &= \frac{4\pi P_2 L_x}{L_y^2} \sin \frac{2\pi}{L_y} y \cos(2\omega t + \theta_2) \end{aligned} \quad (5B.4)$$

Eq.(5B.4) can be written as a Fourier series and the Fourier coefficient,  $a_m$ , is found by an integration procedure evaluated in the interval 0 to  $L_y$ . The result is

$$\begin{aligned} a_m &= -\frac{1}{\pi} \left\{ \frac{\cos(2-m)\pi}{(2-m)} + \frac{\cos(2+m)\pi}{(2+m)} - \frac{1}{(2-m)} - \frac{1}{(2+m)} \right\}, m \neq 2 \\ a_0 &= 0.0 \\ a_2 &= 0.0 \end{aligned} \quad (5B.5)$$

Recalling the Eq.(4.24), the first-order perturbation correction for (0,2,0) mode is

$$p' = - \frac{4\pi P_2 L_x}{L_y^2} \frac{a_0}{(\frac{2w}{c_0})^2 L_x} (2)(-1)^1 S_{100}(1,0,0/2w, \theta_2 + \sigma_{100}) \quad (5B.6)$$

and the total acoustic pressure associated with angular frequency  $2w$  in the cavity becomes

$$p = (0,2,0/2w, \theta_2) - \frac{4\pi P_2}{L_y^2} \frac{a_0}{(\frac{2w}{c_0})^2} (2)(-1)^1 S_{100}(1,0,0/2w, \theta_2 + \sigma_{100}) \quad (5B.7)$$

since  $a_0 = 0.0$

$$p = (0,2,0/2w, \theta_2) \quad (5B.8)$$

According to the calculation developed above there is no need to make a first-order perturbation correction to the (0,2,0) mode in the cavity shown in Fig.4. As a result, the pressure distribution is equal to the second harmonic of the driven mode, since  $a_0 = 0.0$  and this yields  $p' = 0.0$



### C. CAVITY WITH WEDGED PERTURBATION

Under the same assumptions made in sections A and B, assume that the cavity is perturbed as shown in Fig.5 below.

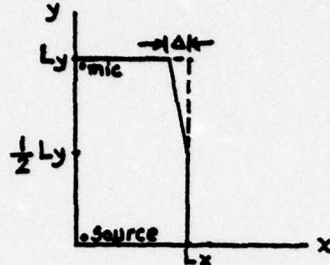


FIGURE 5

The equation for this perturbation is

$$x = L_x \left[ 1 - \frac{\Delta}{L_x} \left( \frac{2y}{L_y} - 1 \right) \right] \quad (5C.1)$$

By means of Eq.(4.8)  $\epsilon$  and  $f(y,z)$  can be written as

$$\epsilon = \frac{\Delta}{L_x} \quad (5C.2)$$

and

$$\begin{aligned} f(y,z) &= 0.0 & , y \leq L_y/2 \\ &= -\left(\frac{2y}{L_y} - 1\right) & , y \geq L_y/2 \end{aligned} \quad (5C.3)$$

Applying exactly the same procedure followed in section A, the total pressure amplitude in the cavity(in first-order perturbation) is

$$P \Big|_{\text{mic. position}} = P_2 \sqrt{(1 + B \cos \sigma_{100})^2 + (B \sin \sigma_{100})^2} \quad (5C.4)$$

where

$$B = \frac{1}{2\pi} \partial_0 \epsilon Q_{100} \sin \sigma_{100}$$

$\sin \sigma_{100}$  and  $\cos \sigma_{100}$  are given by Eq.(5A.21) and (5A.16) respectively.

The theoretical predictions of these specific examples were examined with series of experiments developed by [8].

The further discussions about these will be given in the next section.

## 6. RESULTS

In this section the theoretical predictions performed in sections 5A, 5B and 5C will be compared to the experimental results obtained by [8].

The information on the empirical losses and resonance frequencies is contained in the Q's and e's. These are the values used in the computer program to predict the harmonic distortion on the basis of Eq.(2.16) and is plotted as thin solid curves. The results of including the first-order perturbation correction are plotted as thick solid curves for each specific example. The theoretical curves in figures 6 through 16 were plotted along with the experimentally-measured values for the cavity configurations shown on top of each figure. The theoretically-predicted values were generated for frequency-parameter intervals of 0.2, and the experimentally-measured values were plotted as square-blocks. Data were taken, and theoretical predictions made, for different strength parameters for the (0,n,0) mode associated with different cavity configurations. It is important to note that the n=2 distortion peaks when the system is driven at this frequency. That is, when the driving frequency  $w$  is equal to  $(1/2) w_2$ , there is maximum content of  $P_2$ . The point where this occurs for each  $P_n/P_1$  curve is indicated by <sup>an</sup>  $\nearrow$  arrow with the label of  $F_{020}$ . At that point the value of frequency parameter is

$$F_{020} = 2 Q_{010} e_{020}$$

(The same thing could be done, of course, for any member

of the (0,n,0) family). The arrow labelled as  $F_{100}$  indicates the position where the nearly degenerate (1,0,0) mode is resonant, and the value of  $F_{100}$  is

$$F_{100} = 2 Q_{010} e_{100}$$

The theoretical predictions made in section 5B were compared to the experimental results as seen in Fig.7. When Fig.7 is compared to Fig.6, the unperturbed cavity, it is clearly seen that the theory and experiment are excellently in agreement.

For a wedged perturbation, the theory predicts the frequency of the second harmonic at which the effect of the perturbation occurs as seen in Fig.8. The predicted magnitude of the perturbation effect for this configuration is in good agreement with the experiment. The anomalous behavior of the third harmonic in Fig.8 is unexplained.

For stepped perturbation, when the cavity is perturbed, but the geometry leads to no predicted correction as seen in Fig.9 or leads to predicted correction less than about 0.02 as in Fig.12 or less than about 0.05 as in Fig.14, then it was observed that there was very little or no effect from the (1,0,0) mode. Agreement for these cases is good except for the region lying between frequency parameter 4 and 9 in Fig.9. What happened in that region is also unexplained, but it was observed one time only. When the amount of perturbation correction is increased the theory predicts effects larger than experimentally observed. However, the effect of the perturbation appears at the right frequency



parameter as is seen in Fig.'s 10,11,13,15 and 16.

Choosing the shim position, length and magnitude is very important as well as is choice of the strength parameter.

For the shims,  $\Delta=0.04$  and 0.25 inches for stepped and wedged perturbations respectively. The effect of strength parameter can be seen in Fig.'s 15 and 16. The experimental data associated with the third harmonic in Fig.15 were believed to come from harmonic distortion in the piston motion.

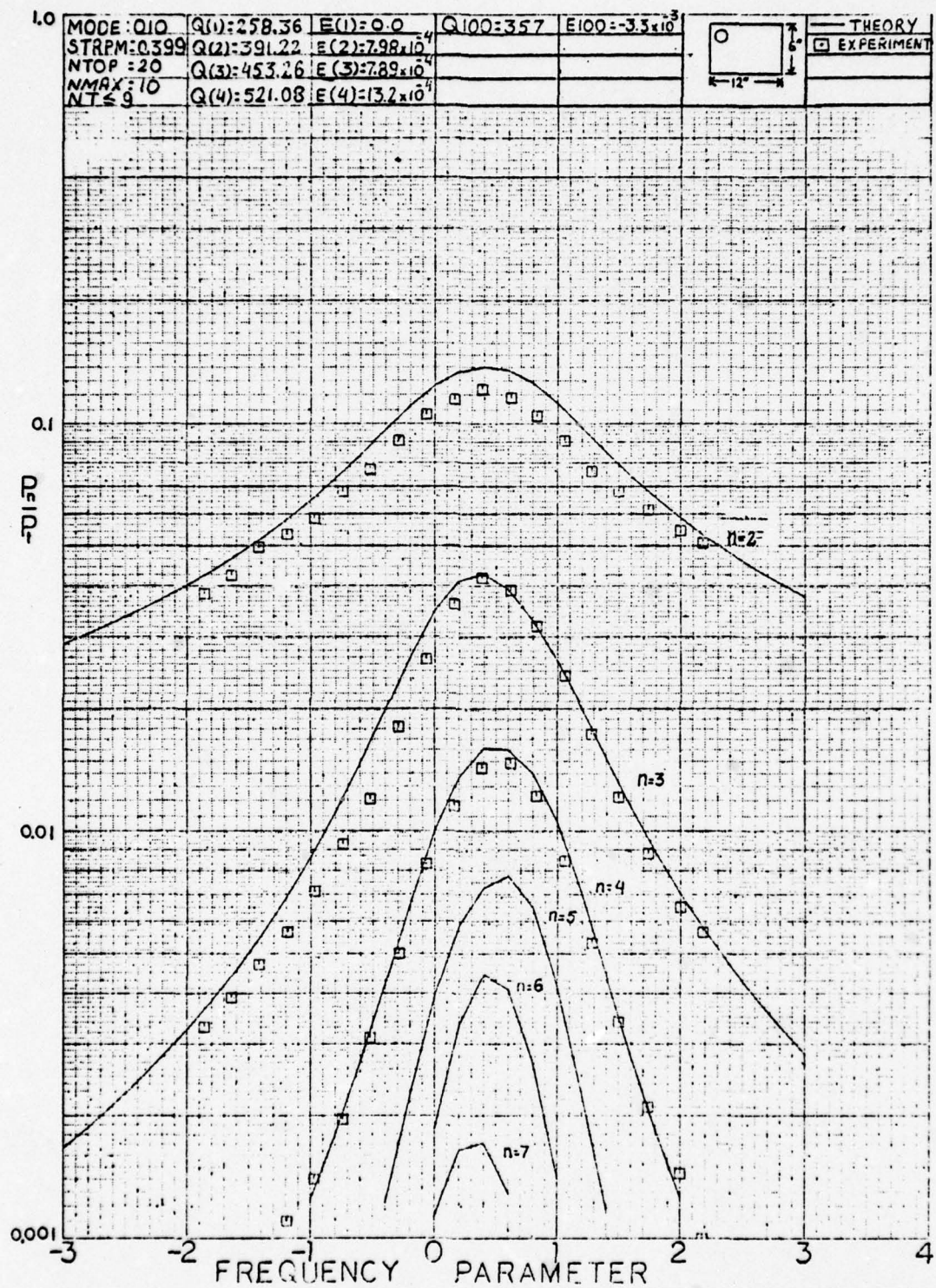


FIGURE 6



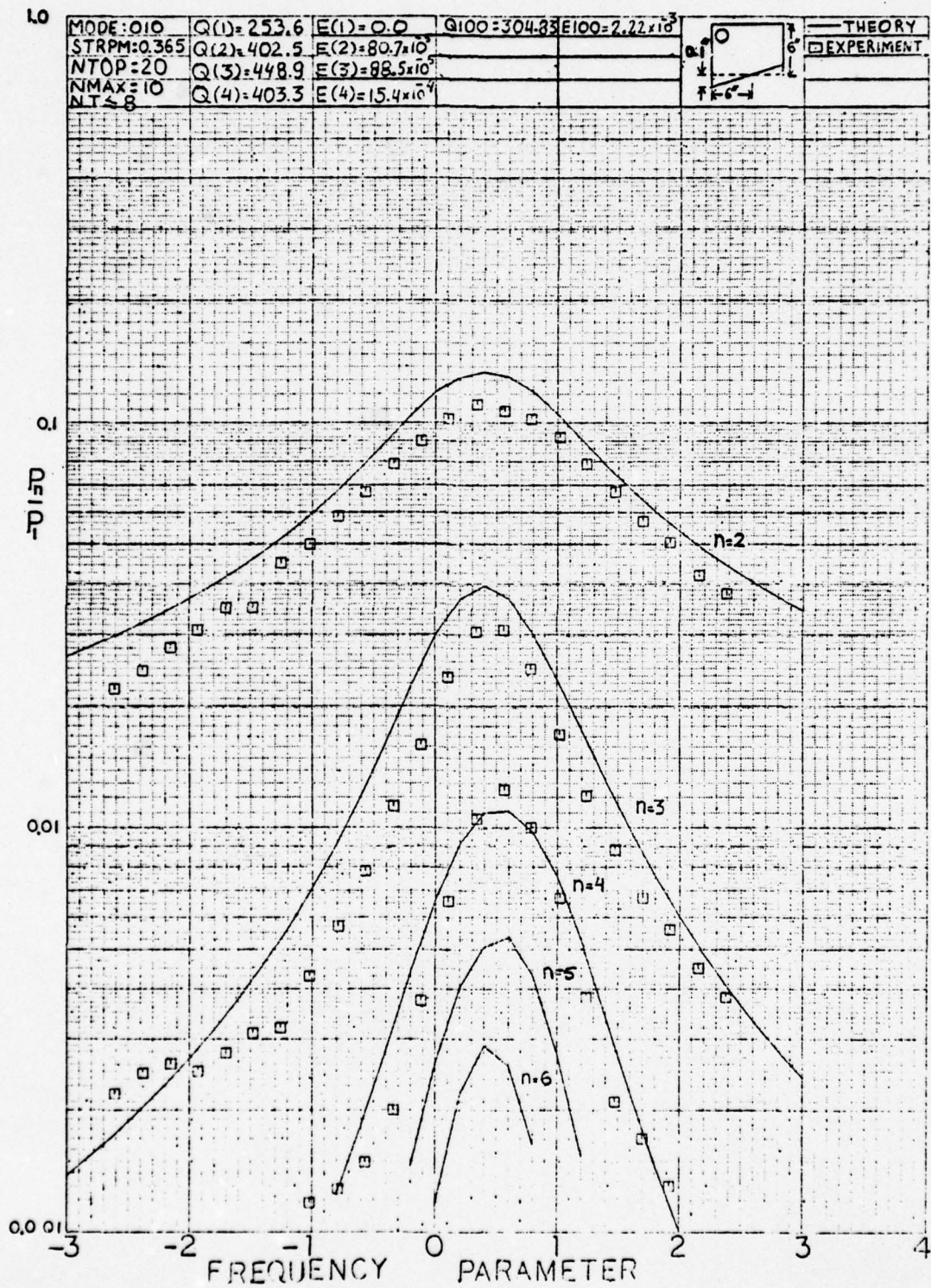


FIGURE 7



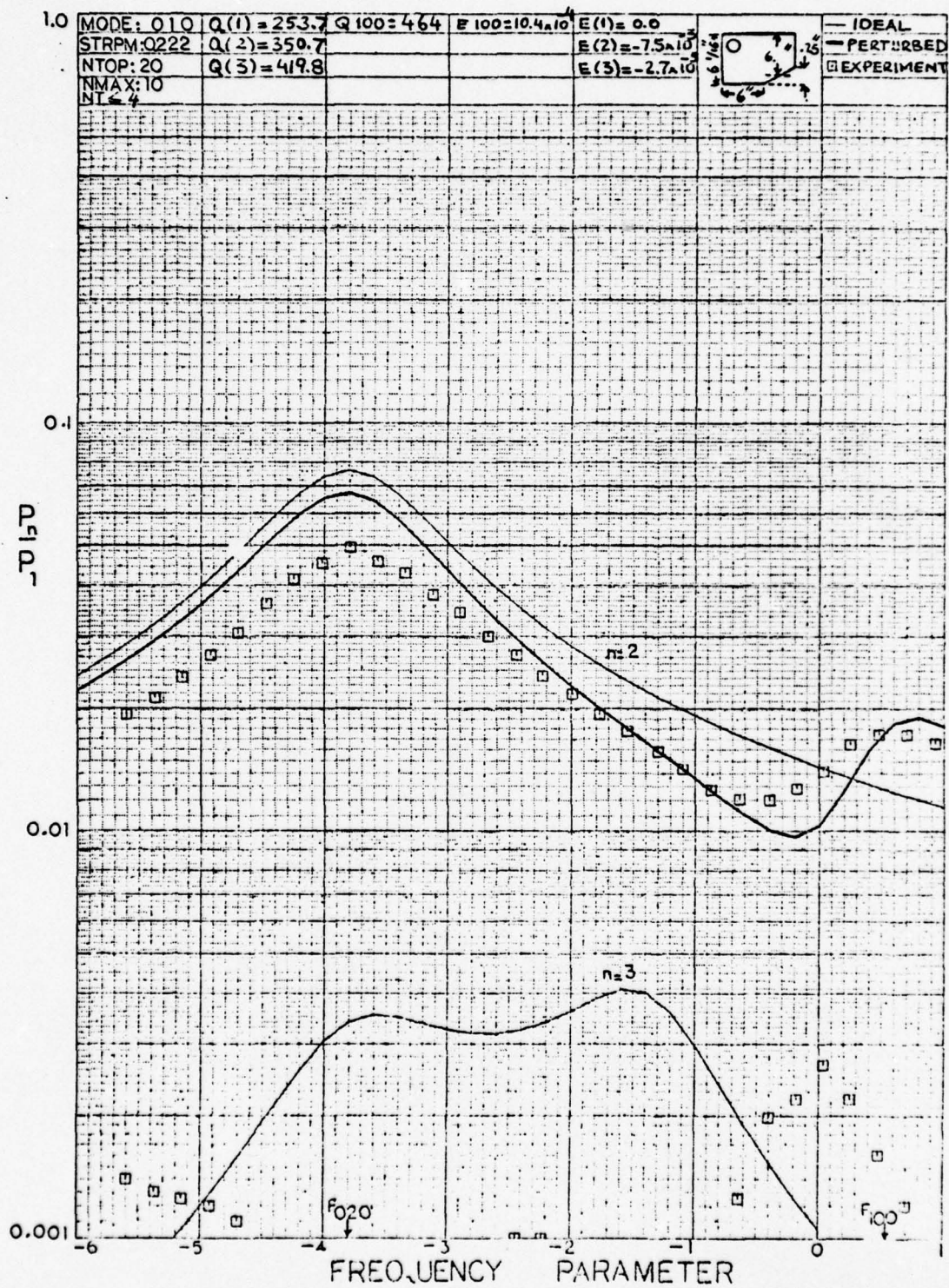
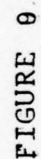


FIGURE 8





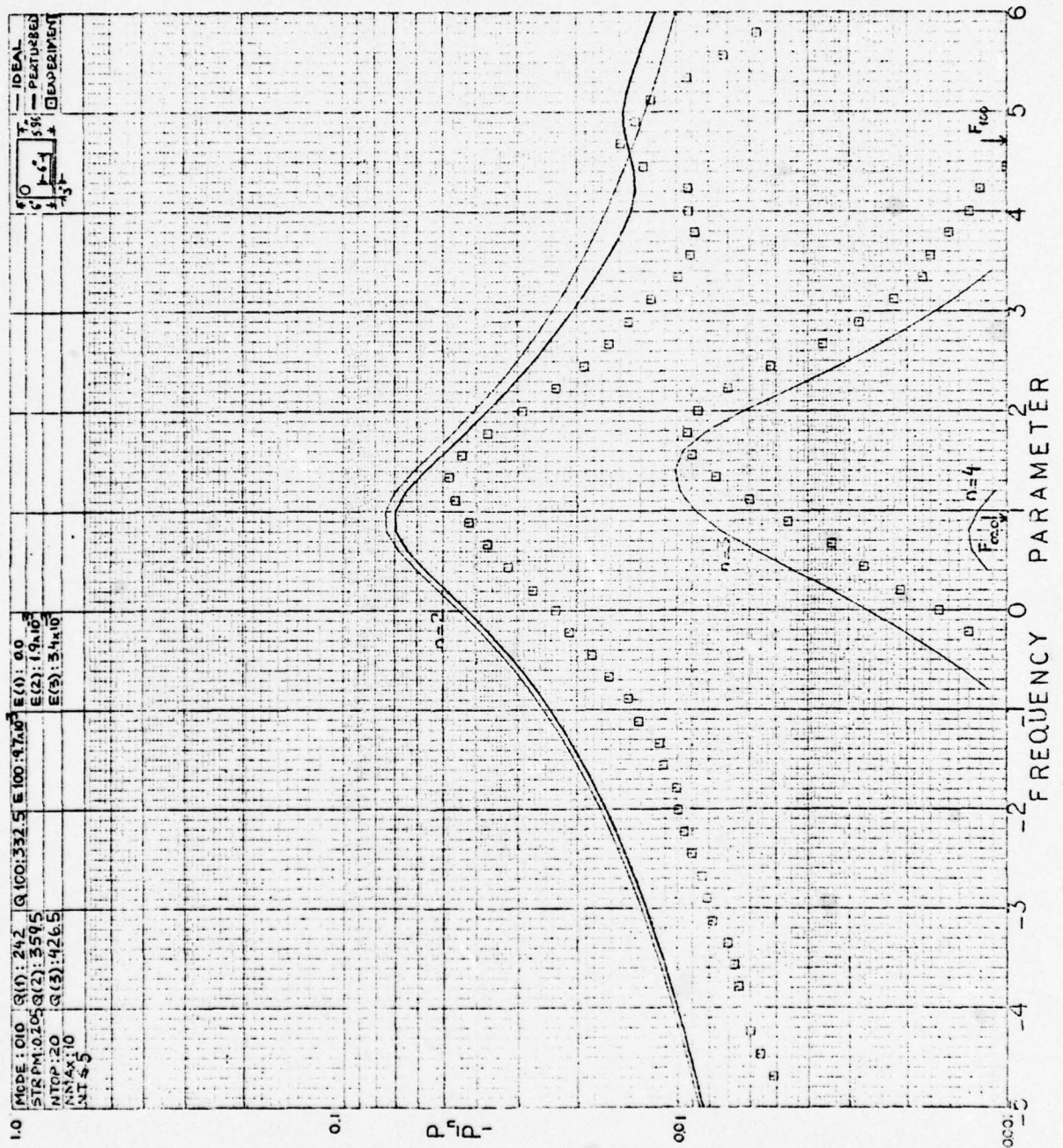


FIGURE 10



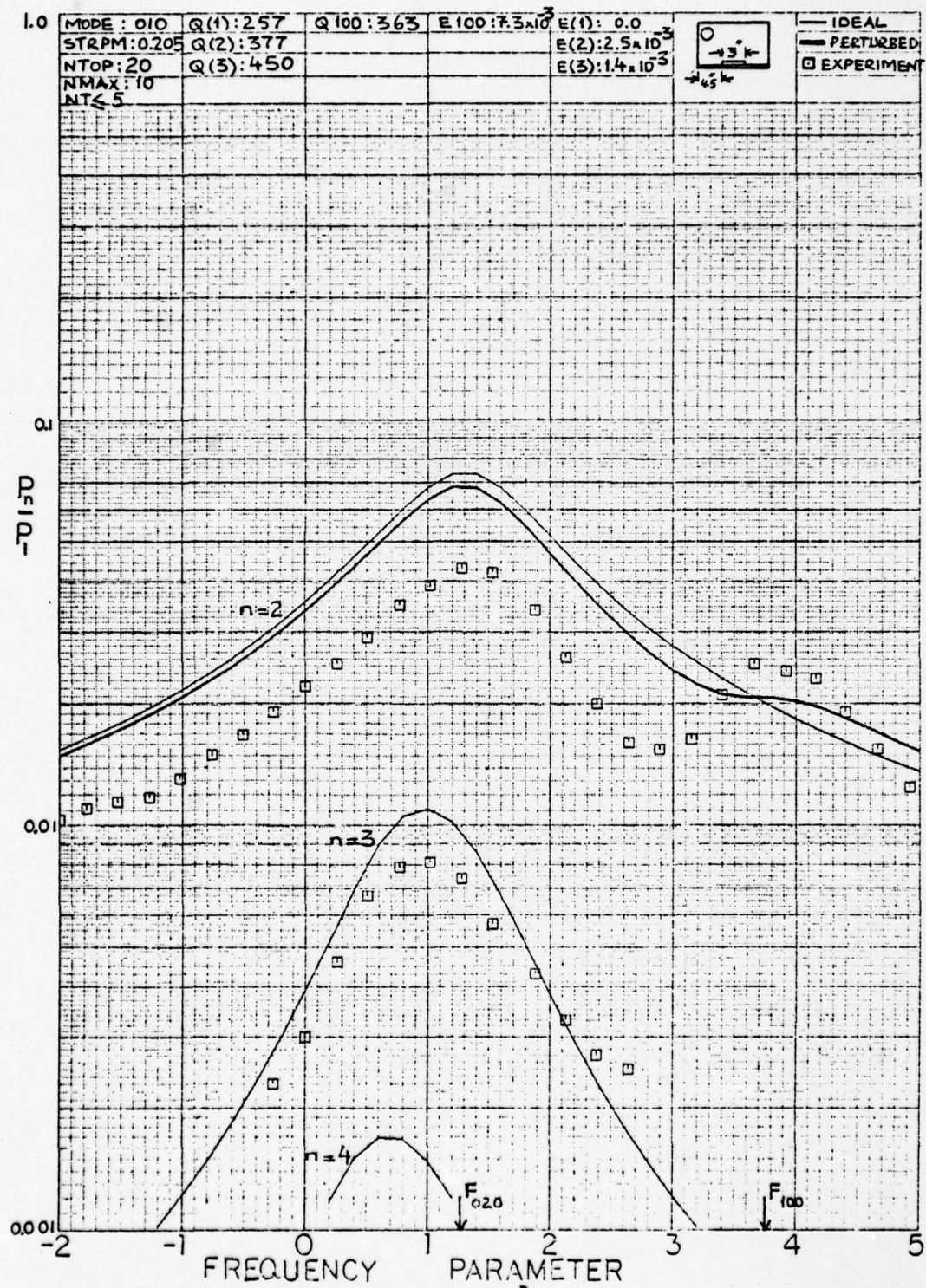


FIGURE 11

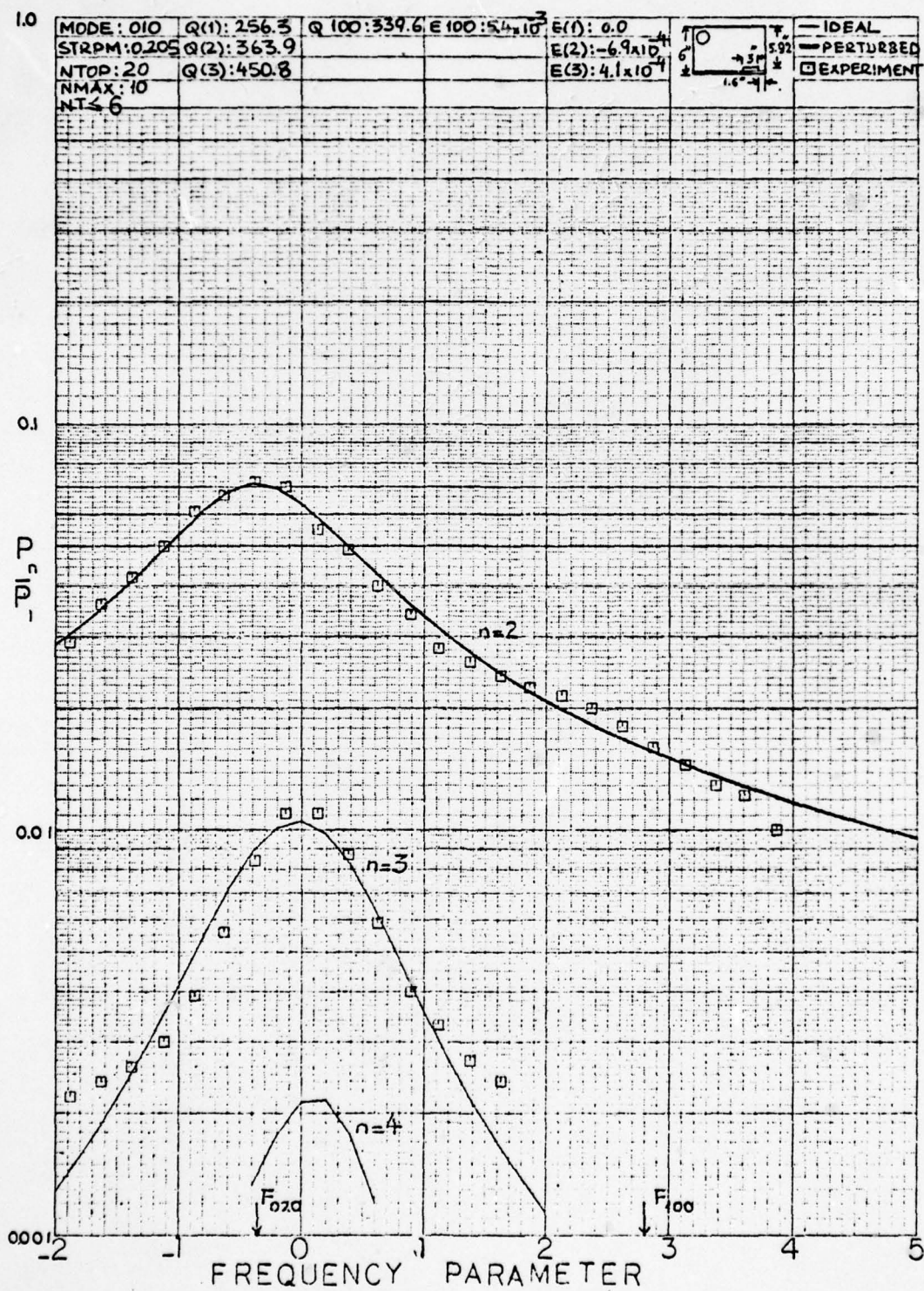


FIGURE 12



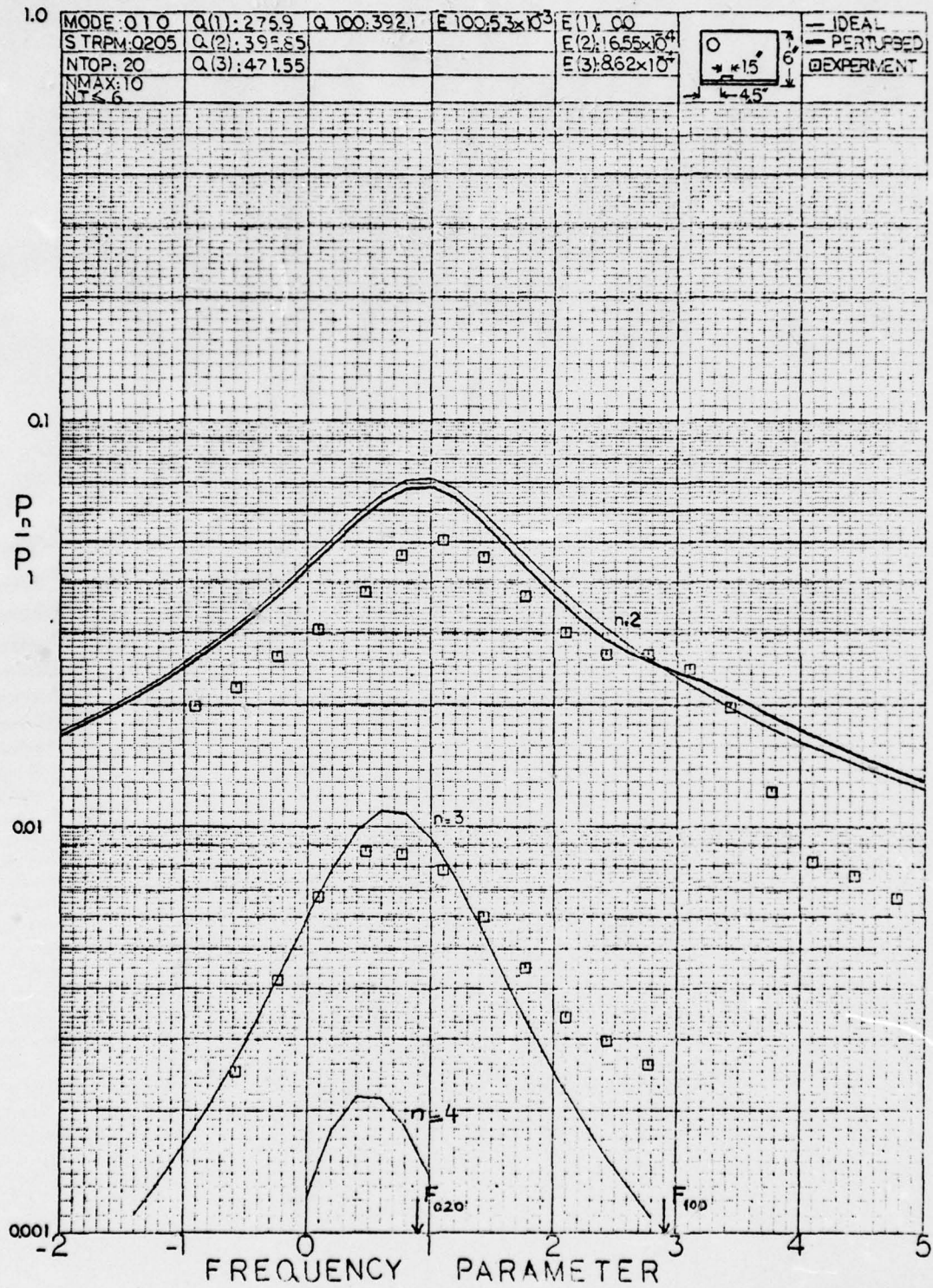


FIGURE 13



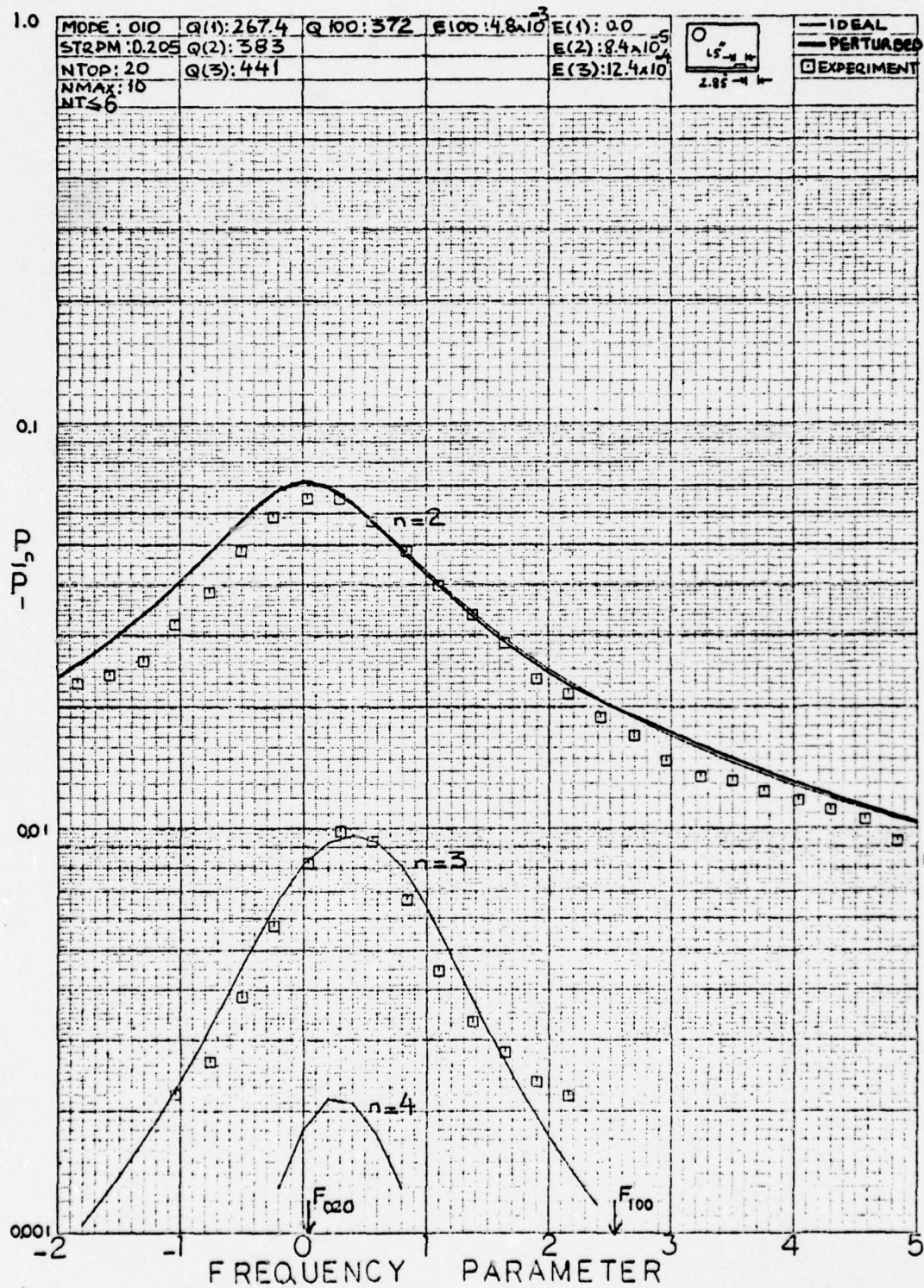


FIGURE 14

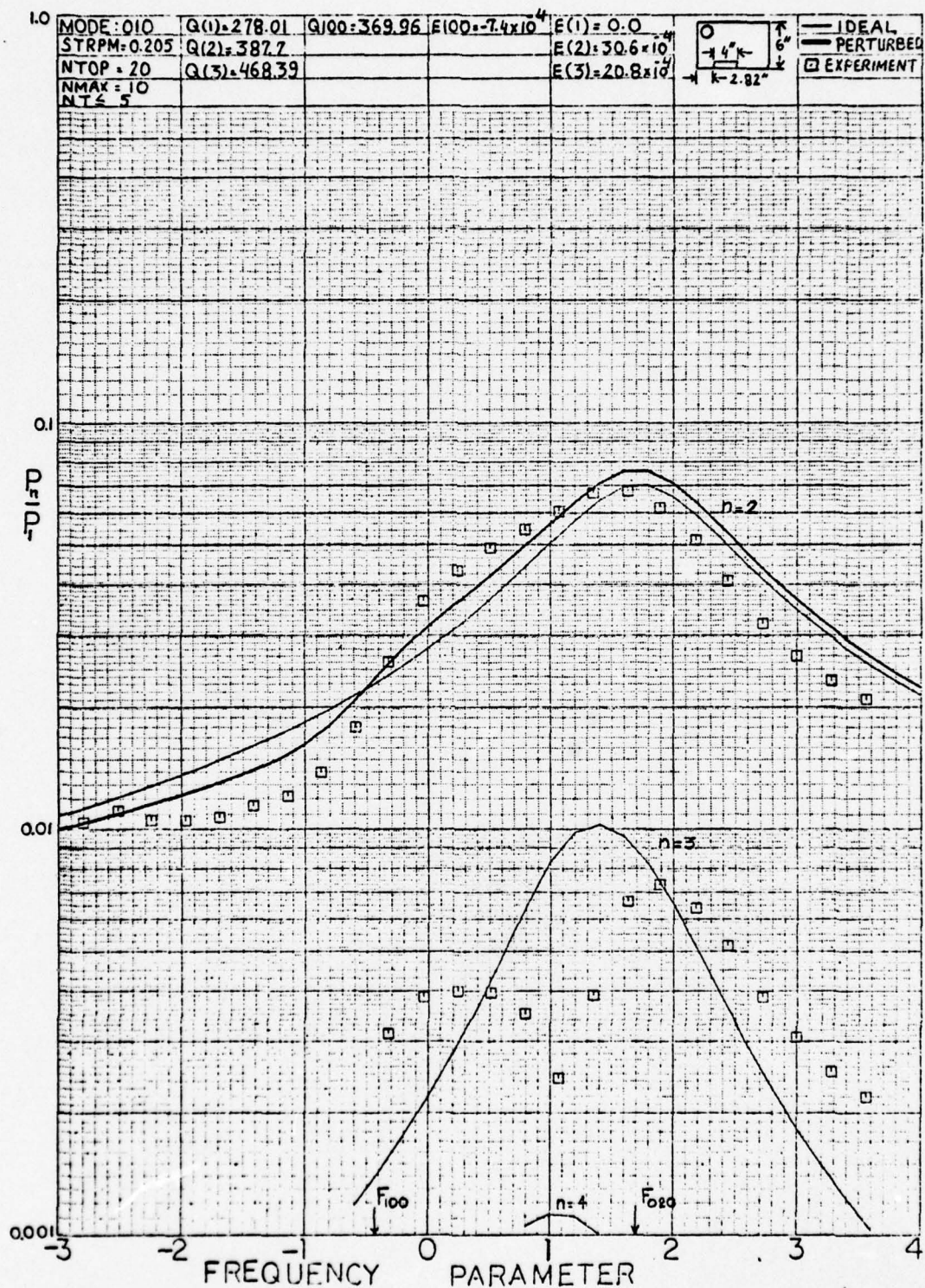


FIGURE 15



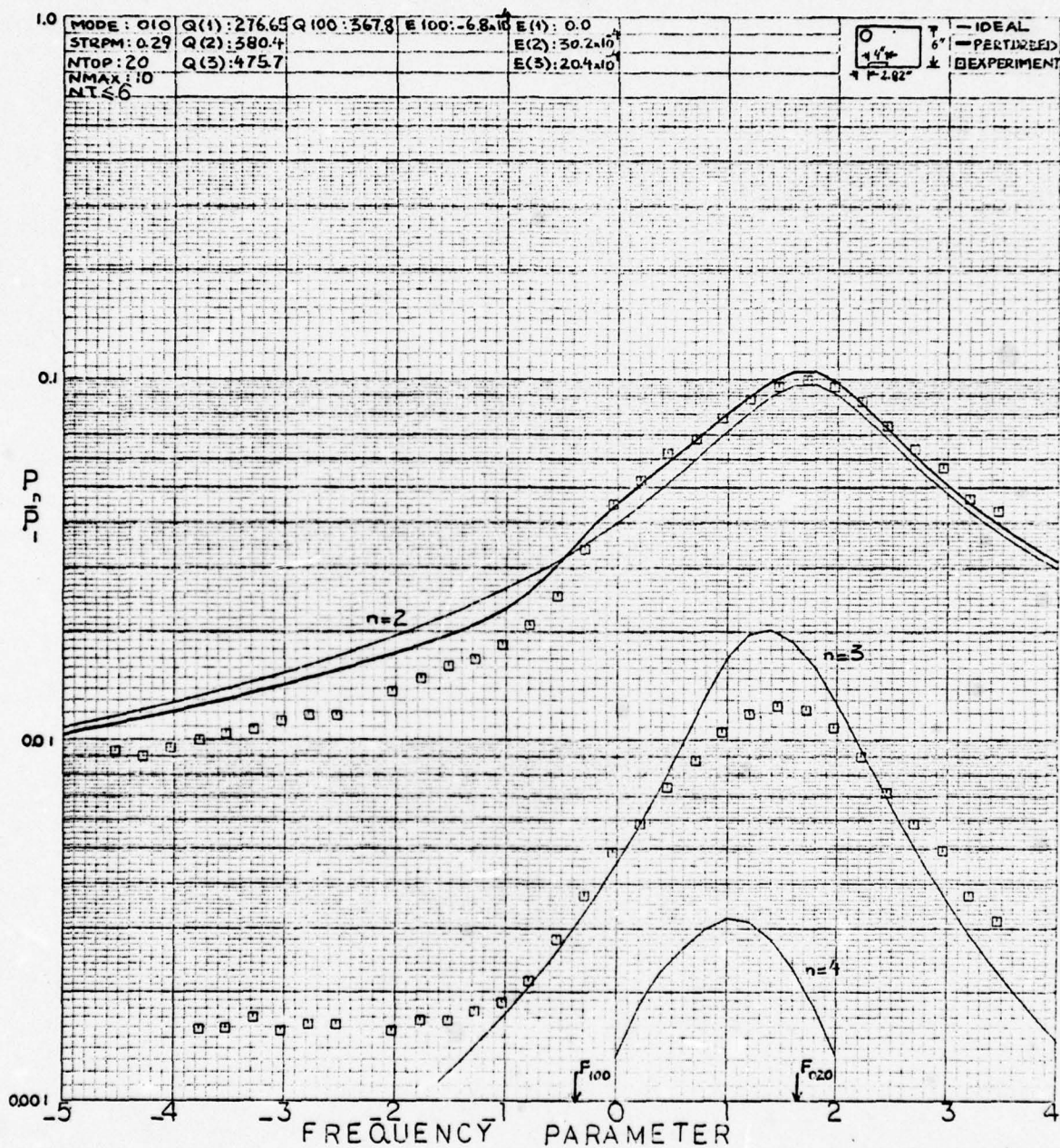


FIGURE 16



## 7. CONCLUSION

Non-linear theory has been applied to standing waves in a rigid-walled rectangular cavity with a perturbed boundary in order to find one possible mechanism for the excitation of a standing wave other than those belonging the family of the driven mode. It was observed that such an excitation exists if the boundary perturbation and the dimensions of the cavity are favorably chosen.

It appears that the present theoretical model successfully predicts the major features of harmonic content for finite-amplitude standing waves in the cavity when the geometry leads to no perturbation correction (Fig. 7 and 9). When the magnitude of the perturbation is increased the predicted features were larger than experimentally observed. Second-order perturbation corrections may be needed to account for these discrepancies.

## APPENDIX A

The original computer program for Eq.(2.16) was prepared by Coppens in 1973, and author made some extentions to that program so that it would (1) calculate the perturbation correction and (2) present the results graphically. The program calculates the relative amplitudes and phase angles of standing waves in cavities keeping the strength parameter constant and changing the frequency parameter to generate response curves showing the amplitudes of the nonlinearly excited standing waves as function of the frequency parameter  $F_1$ . It also calculates the perturbation correction according to Eq.(4.24) and then finds the total relative pressure amplitude using Eq.(4.26). The program also draws the graph of the relative pressure amplitudes of the ideal cavity, total relative pressure amplitude of the perturbed cavity and the experimental data on a 3 cycle semilog paper. The Versatec Graphics Plotting Manual [10] was used for the graphical processes on the IBM 360 of the Randolph Church Computer Center, Naval Postgraduate School.

## SOME USEFUL INFORMATION ABOUT COMPUTER PROGRAM

\* Quantities marked with (\*) must be controlled or changed for each run.

\*KON           The number of iterations throughout the region of interest. For this program the iterations are performed with 0.2 intervals.

\*NCUR           The number of the experimental curves to be drawn + 1

\*NDAT           The number of experimental data in the region of interest

BUR(I,J)       The array that stores the experimental data

\*XL            The length of the cavity in the x-direction

\*YL            The length of the cavity in the y-direction

\*DELTA          The magnitude of the perturbation

\*STRPM          Strength parameter

\*FREQ           Frequency parameter stored in ATA(I,1) and ZER(I,1). Input as the maximum value of FREQ in the region of interest

XDAT(JET)       The x coordinate

YDAT(JET)       Value of the curve  $f(x)$  for XDAT

ATA(I,N), N#1   The array that stores the logarithmic value of the pressure amplitudes of the harmonics of the driving mode

ZER(I,N), N#1   The array that stores the linear value of the pressure amplitudes of the harmonics of the driving mode

\*Q(I)           Quality factors of driving mode and harmonics of it

\*E(I)           e's value of driving mode and harmonics of it



\*Q100            Quality factor of (1,0,0) mode

\*E100            e-value of (1,0,0) mode

\*XDAT(JET+1) Integer value of left-hand corner on the x-axis.  
It must have the same value as the 7th argument  
of subroutine CALL AXIS for x-axis.

\*YDAT(JET+1) Integer value of left-hand corner on the y-axis.  
It must have the same value as the 7th argument  
of subroutine CALL AXIS for y-axis.

XDAT(JET+2) }  
                      Increment value of x and y for scaling purposes  
YDAT(JET+2) }

HUM            The linear value of the total acoustic pressure  
                 amplitude associated with angular frequency  $2w$ .

\*B             $\frac{\epsilon}{\pi} Q_{100} \sin \sigma_{100}^{(1/4)} L_y a_0$  for stepped perturbation  
                  $\frac{\epsilon}{\pi} Q_{100} \sin \sigma_{100}^{(a_0/2)}$  for wedged perturbation  
                 and  $a_0$  is the 0th Fourier coefficient.

```

// EXEC FORTCLGW
// FORT.SYSIN DD *
-----
STANDING WAVES IN CAVITIES-----
NO DATA READIN-----TO START OFF ON SKIRTS
AND GENERATE A STARTING RAMP(N) AND PHI(N) FOR
THIS PROGRAM CALCULATES RAMP(N) AND PHI(N) FOR
STANDING WAVES IN THREE DIMENSIONAL CAVITIES
THE PROGRAM KEEPS STRPM THE SAME BUT
CHANGES FREQ TO GENERATE A RESPONSE CURVE
-----
DIMENSI ON RAMP(50), PHI(50), THETA(50), FAC(50), S(50), C(50),
2 RATIO(50), DPHI(50), FIX(50), E(50), Q(50), CCRP(50), CCRR(50),
3 ZER(62,10), BUR(62,10), Y(200), V(100), XDAT(62), YDAT(62), ATA(62,10)
DATA LMASK1/-30584/, LMASK2/-21846/
DATA ZER, BUR, ATA/1860*0./
DATA Y, V/300*0./
DATA XDAT, YDAT/124*0./
R=10./3.
L=0
K=0
KON=36
1 FORMAT(/33X,'STRENGTH PARAMETER =',F5.3,
/33X,'FREQUENCY PARAMETER =',F6.3,
/33X,'N TOP =',I5,
/33X,'N MAX =',I5,
/33X,'N T =',I5//)
2 FCRMAT(17X,15,4,F15.4)
3 FCRMAT(17X,15,4,F15.4)
4 FCRMAT(17X,15,4,F15.4)
5 FCRMAT(17X,15,4,F15.4)
6 FCRMAT(17X,15,4,F15.4)
7 FCRMAT(17X,15,4,F15.4)
8 FCRMAT(17X,15,4,F15.4)
9 FCRMAT(17X,15,4,F15.4)
10 FCRMAT(17X,15,4,F15.4)
11 FCRMAT(17X,15,4,F15.4)
-----
DO 475 READS THE EXPERIMENTAL DATAS WITH FORMAT 1001
NCUR=NUMBER OF CURVES TO BE DRAWN+1
-----
NCUR=3
NDAT=24
DC 475 1=1,NDAT
475 READ(5,1001) (BUR(I,J),J=1,NCUR)

```

```

1001 FC RMAT (4F8.6)
DO 50 N=1,50
  F1X(N)=0.0
  RAMP(N)=0.0
  PHI(N)=0.0
  RATIO(N)=0.0
  CPHI(N)=0.0
  THETA(N)=0.0
  FAC(N)=0.0
  CORR(N)=0.0
  S(N)=0.0
  C(N)=0.0
  E(N)=0.0
  Q(N)=0.0
  QNT=1
  PI=3.14159
  RAMP(1)=1.0
  PHI(1)=0.0
  S(1)=0.0
  C(1)=1.0

```

50

C

```

-----
INPUT VALUES FOR PERTURBATION CORRECTION
Q100=339.6
E100=5.43E-3
XL=5.96
YL=12.0
DELTA=0.04

```

C

```

-----
INPUT PARAMETERS
RECTANGULAR CAVITY
FAMILY OF MODES GIVEN BY VALUE OF RELABS
KEEP NTOP, NMAX LE 50

```

```

RELABS=0.205
STPRM=0.205
FREQ=5.2
NMAX=10
NTOP=20
EXMIN=0.75

```

C

```

E-4 THRU 90 CALCULATES INFINITESIMAL-AMPLITUDE
RESNANCE PARAMETERS FOR NON-R-K CASE
Q(1)=256.25
Q(2)=363.85
Q(3)=450.8
E(1)=0.0
E(2)=-6.85E-4
E(3)=4.085E-4

```



```

CC 89 N=4,NMAX
XA=FLOAT(N)
Q(N)=Q(1)*SCRT(XN)
E(N)=0.501*COS(XN-5.0)
85 CONTINUE
WR=TE(6,11)(N,Q(N),E(N),N=1,NMAX)
DC 400 LS=1,KON
FRUP=FREQ-J.2
DC 50 N=1,NMAX
TEMP=2.0*E(N)*Q(1)
XNUM=-FRUP+TEMP
XNBF=-FREQ+TEMP
XDEN=C(1)/Q(N)
XD2=XDEN*XDEN
TEMP=SQRT(XNUM**2+XD2)
TNBF=SQRT(XNBF**2+XD2)
THETA(N)=ATAN2(XNUM,XDEN)
ARGN=XNUM-XNBF
ARGD=XDEN+(XNUM*XNBF/XDEN)
CORP(N)=ATAN2(ARGN,ARGD)
CCRR(N)=TNBF/TEMP
FAC(N)=0.5*STRPM/TEMP
FREQ=FRUP
SC
-----
HERE THROUGH 383 INITIALIZES RATIO(N) AND DPHI(N)
DO 380 CALCULATES INITIAL VALUES FOR RATIO(N) AND DPHI(N)
AND OBTAINS THE VALUE OF N=NT AFTER WHICH RATIO=0.0 AND
RAMP LE RMIN
NT=NMAX
T1=1.0
T2=0.0
DC 380 N=2,NMAX
IF(RAMP(N)-RMIN)365,369,370
369 NT=N-1 J=N,NMAX
RATIO(J)=0.0
DFF1(J)=0.0
GO TO 383
370 RATIO(N)=(RAMP(N)/RAMP(N-1))*0.5*(1.0+CORR(N))
C1FF=PHI(N)-PHI(N-1)
IF(ABS(D1FF)-PI)374,371,371
IF(D1FF-PI)373,372,372
D1FF=D1FF-2.0*PI
GO TO 374
D1FF=D1FF+2.0*PI
C1FF1(N)=D1FF+CORP(N)
T1=T1+RATIO(N)
T2=T2+DPHI(N)
373
374

```

52

```

      XN=FLOAT(N)
      TEMP=1.0/XN
      RATIO(N)=RINF-RSLP*TEMP
      DPHI(N)=DPINF-DSLPL*TEMP
      CONTINUE
80 CONTINUE
81 DC 300
      LM=2.50
      HERE THRU 278 CALCULATES RAMP(N) AND PHI(N) FROM
      N=(LP LE NMAX), (NT-1) AND EXTRAPOLATES THEM FROM
      N=NT, NTCF. ALL RAMP AND PHI BEYOND RAMP(N)=RMIN
      ARE SET TO 0.0. THE ASSOCIATED S(N) AND C(N) ARE FCUND.
      IF(LM-NMAX)260,260,261
260 LP=LM
      GC TO 262
261 LF=NMAX
262 DO 276 N=LP,NTOP
      IF(RAMP(N-1)-RMIN)270,270,271
273 DC 277 J=N,NTOP
      RAMP(J)=0.0
      PHI(J)=0.0
      S(J)=0.0
      C(J)=0.0
      GC TO 278
271 RAMP(N)=RAMP(N-1)*RATIO(N)
      PHI(N)=PHI(N-1)+DPHI(N)
      IF(ABS(PHI(N))-PI)275,272,272
272 IF(PHI(N)-PI)274,273,273
273 PHI(N)=PHI(N)-2.0*PI
      GC TO 275
274 PHI(N)=PHI(N)+2.0*PI
275 S(N)=RAMP(N)*SIN(PHI(N))
      C(N)=RAMP(N)*COS(PHI(N))
      CONTINUE
276 CONTINUE
      HERE THRU 300 CALCULATES NEW VALUES
      OF FIX(N) FOR N=1,LP
      XLM=FLOAT(LM)
      DO 300 N=1,LP
      XN=FLOAT(N)
      FIX(N)=FXMX/(XLM-XN+1.0)
      CONTINUE
300 CONTINUE
      HERE THRU 131 CALCULATES NEW VALUES FOR RAMP(N),
      PHI(N), S(N), AND C(N) FOR N=2,LP. WHEN
      (RAMP(N)-RMIN), THEN FOR (IN LE N LE LP) ALL
      ARE SET TO ZERO
      DC 100 N=2,LP
      SUMC1=0.0
      SUMC2=0.0

```



```

SUMS1=0.0
SUMS2=0.0
M=N-1
IF(M) 105,105,102
102 DO 104 J=1,M
K=N-J
SUMS1=SUMS1+S(J)*C(K)+C(J)*S(K)
104 SUMC1=SUMC1+C(J)*C(K)-S(J)*S(K)
105 M=NTOP-N
IF(M) 109,109,106
106 DO 108 J=1,M
K=N+J
SUMS2=SUMS2+S(K)*C(J)-C(K)*S(J)
108 SUMC2=SUMC2+C(K)*C(J)+S(K)*S(J)
F=0.5*SUMS1-SUMC2
G=0.5*SUMC1-SUMC2
TEST=F*2+G*2
RAMP(N)=RAMP(N)+FIX(N)*(FAC(N)*SQR(TTEST)-RAMP(N))
110 IF(RAMP(N)-RMIN) 110,111,111
DC 131 J=N,LP
RAMP(J)=0.0
PHI(J)=0.0
S(J)=0.0
SC(J)=0.0
131 GO TO 58
111 TEST=ATAN2(F,G)
TEST=PI-TEST+THETA(N)-PHI(N)
122 IF(ABS(TEST)-PI) 123,123,123
123 IF(TEST-PI) 124,124,124
TEST=TEST-2.0*PI
124 GO TO 113
TEST=TEST+2.0*PI
113 PHI(N)=PHI(N)+FIX(N)*TEST
27 IF(ABS(PHI(N))-PI) 28,28,28
28 IF(PHI(N)-PI) 29,29,29
29 PHI(N)=PHI(N)-2.0*PI
GO TO 129
PHI(N)=PHI(N)+2.0*PI
129 S(N)=RAMP(N)*SIN(PHI(N))
100 C(N)=RAMP(N)*COS(PHI(N))
58 CONTINUE
300 CCONTINUE
THRU 183 CALCULATES NEW RATIO(N) AND DPHI(N)
FOR ALL NONZERO RAMP(N). RAMP(N) IS HIGHEST
NONZERO RAMP, BUT NT IS NEVER GREATER THAN NMAX.
RATIO(N) AND DPHI(N) ARE SET TO ZERO FOR
(NT LE NMAX)
NT=NMAX
CCCCC

```

```

165      CG 180 N=2 NMAX
      IF (RAMP(N)) 169,169,170
      NT=N-1
      DC 182 J=N,NMAX
      RATIO(J)=0.0
      DPHI(J)=0.0
      GO TO 183
170      RATIO(N)=RAMP(N)/RAMP(N-1)
      DIFF=PHI(N)-PHI(N-1)
      IF (ABS(DIFF)-PI) 174,171,171
171      IF (DIFF-PI) 173,172,172
172      DIFF=DIFF-2.0*PI
      GO TO 174
173      DIFF=DIFF+2.0*PI
174      DPHI(N)=DIFF
180      CONTINUE
183      CONTINUE
      WRITE(6,11) (N,RAMP(N),PHI(N),N=1,NT)
1000      CONTINUE
      WRITE(6,10)
      WRITE(6,1) STRPM,FREQ,NTOP,NMAX,NT
      WRITE(6,3)
      N=1
      WRITE(6,4) (N,RAMP(N),PHI(N)
      WRITE(6,6) (N,RAMP(N),PHI(N),RATIO(N),DPHI(N),N=2,NMAX)
      ZER(LS,1)=FREQ
      ATA(LS,1)=FREQ
      DC 1789 MEH=2.10
      IF (RAMP(MEH)-LE-9.001) GO TO 1788
      ATA(LS,MEH)=RAMP(MEH)
      ZER(LS,MEH)=R*ALOG10(RAMP(MEH)*1000.0)
      M=NMAX+1
      WRITE(6,4) (N,RAMP(N),PHI(N),N=N,NTOP)
      WRITE(6,9)
      WRITE(6,2) NT,RINF,RSLP,DPINF,CSLP
      WRITE(6,10)
4000      CONTINUE
      C STARTING TO DRAW A SEMI-LOG(3*70) GRAPH AS A BACKGROUND
      CALL PLOTS(0,0)
      CC 1111 I=1,3
      Z=1.0
      DO 2222 J=1,60
      K=K+1
      IF (Z-GE-4.0) GO TO 3333
      Y(K)=R*(ALOG10(Z+.1)-ALOG10(Z))
      Z=Z+.1
      GO TO 2222
3333      Y(K)=R*(ALOG10(Z+.2)-ALOG10(Z))

```





```

1784 C      CALL LINE(XCAT,YDAT,JET,1,-1,0)
      CGNTINUE
      STARTING TO DRAW PERTURBATION CORRECTION
      ZIR=2.*Q(1)*E100
      ZOR=1.-E100
      ZAR=Q(1)*Q(1)
      EPSILO=DELTA/XL
      JET=0
2950 DC 2950 I=1,KCN
      IF(ATA(I,2).EQ.0.) GO TO 2950
      JET=JET+1
      SINSIG=1./SQRT(1.+(ZAR*(ATA(I,1)-ZIR)*ZOR)**2)
      CCSSIG=SQRT(1.-SINSIG**2)
      IF(ATA(I,1).LE.ZIR) CCSSIG=-CCSSIG
      B=(0.037*EPSILO*Q(1)*SINSIG)/PI
      HUM=ATA(I,2)*SQRT((1.+B*CCSSIG)**2+(B*SINSIG)**2)
      YDAT(I)=R*ALOG10(HUM*1000.)
      XCAT(I)=ATA(I,1)
2950 CGNTINUE
      XCAT(JET+1)=-2
      XDAT(JET+2)=1.
      YDAT(JET+2)=0.0
      CALL NEWPEN(3)
      CALL LINE(XCAT,YDAT,JET,1,0,0)
      CALL PLOT(0,0.,+999)
      WRITE(6,2951)
2951 FORMAT(1,1,20X,'FREQ. PARAM. P(2)/P(1) P(3)/P(1) P(4)/P(1)
      DC 2952 I=1,KCN
      WRITE(6,2953) (ATA(I,J),J=1,6)
2953 FORMAT(22X,F5.2,9X,F5.5,6X),/)
      CGNTINUE
      STOP
      END

```

#### BIBLIOGRAPHY

- [1] A.B.Coppens, Private Communication
- [2] A.B.Coppens, Private Communication
- [3] A.B.Coppens, and J.V.Sanders, "Finite Amplitude Standing Waves within Real Cavities", J. Acoust. Soc. Am., 58(6), December, 1975.
- [4] M.J.Kilmer II, Finite Amplitude Effects in Rectangular Cavities with Perturbed Boundaries, Thesis, Naval Postgraduate School, Monterey, California, 1975.
- [5] R.R.DeVall, Finite Amplitude Waves in Imperfect Cavities. Thesis, Naval Postgraduate School, Monterey, California, 1973.
- [6] G.Kirchoff, Ann. Phys. Leipzig, V.134 P.177-193, 1868.
- [7] H.Lamb, Dynamical Theory of Sound 2nd ed., Chap.6, Edward Arnold and Co., London England, 1925.
- [8] E.Kuntsal, Finite Amplitude Standing Waves in Rectangular Cavities with Perturbed Boundaries, Thesis, Naval Postgraduate School, Monterey, California, December, 1978.
- [9] D.T.Blackstock, J. Acoust. Soc. Am. 36, 217(L), 1964.
- [10] Versatec Graphics Plotting Manual, Tech. Note No:0141-34 February, 1978.

INITIAL DISTRIBUTION LIST

	Number of Copies
1. Defense Documentation Center Cameron station Alexandria, Virginia 22314	2
2. Library, Code 0142 Naval Postgraduate School Monterey, California 93940	2
3. Department Library, Code 61 Department of Physics and Chemistry Naval Postgraduate School Monterey, California 93940	2
4. Professor Alan B. Coppens, Code 61 Cz Department of Physics and Chemistry Naval Postgraduate School Monterey, California 93940	2
5. Professor James V. Sanders, Code 61 Sd Department of Physics and Chemistry Naval Postgraduate School Monterey, California, 93940	1
6. LT. Mehmet Aydin Zincirlikuyu Caddesi No=99 Kasimpasa, Istanbul/TURKEY	3
7. LT. Ender Kuntsal Akatlar, Zeytinoglu Caddesi Safak Apt. 240/16 Etiler, Istanbul/TURKEY	1
8. Turk Deniz Kuvvetleri Komutanligi Ankara/TURKEY	2
9. Dr. D. T. Blackstock Applied Research Laboratory University of Texas Austin, Texas 78712	1



10.Dr.Logan Hargrove, Code 421

1

Physics Program, ONR,

Ballston Centre Tower #1,

Quincy Street, Washington DC., 20613